[redacted]

MARTIN MARIETTA ENERGY SYSTEMS LIBRARIES
3 4456 0356246 4

PROVIDE THIS DOCUMENT AS

AEC RESEARCH AND DEVELOPMENT REPORT

APPENDICES

to

CHAPTER III - POWER PLANTS

AEC RESEARCH AND DEVELOPMENT REPORT

NUCLEAR - POWERED FLIGHT

A Report to

THE ATOMIC ENERGY COMMISSION

by

THE LEXINGTON PROJECT

[redacted]

DECLASSIFIED

Classification Cancelled
By Authority of TID-1292 [redacted]
Classification Officer
Date 3-31-64

[redacted]

CHAPTER III

POWER PLANTS

Appendices

A Analysis of Open-Cycle Turbojet

B Analysis of Helium Gas-Turbine Compressor-Jet

C Analysis of Bismuth Turbojet

D Materials for Gas-Turbines and Jet Engines

E Analysis of Reactor Heat Transfer

MARTIN MARIETTA ENERGY SYSTEMS LIBRARIES

3 4456 0356246 4

[redacted]

[redacted]

APPENDIX III

Section A

ANALYSIS OF OPEN-CYCLE TURBOJET

The method used to analyze the performance of the open-cycle turbojet is illustrated by means of a numerical example. Consider a turbojet power plant (see Fig. III-1) operating at 30,000 feet and a flight Mach number of 0.9.

The following assumptions, some of them specific to this particular example, will be made in the analysis:

Atmospheric pressure, density, and temperature are as tabulated in NACA Report No. 218.

The properties of air are as given in "Thermodynamic Properties of Air" by Keenan and Kaye.

The compressor pressure ratio is 40:1.

One intercooler is used with an effectiveness of 0.50 and a pressure drop of 5%.

The turbine inlet temperature is 1800°F (982°C).

The component efficiencies are as follows:

Diffuser	.90
Compressor (temperature-rise efficiency for each unit)	.835
Compressor (adiabatic efficiency of each unit)	.82
Turbine	.87
Exhaust duct and nozzle	.90

At 30,000 feet the atmospheric properties (NACA standard) are:

P_a = Pressure	4.36 psia
ρ_a = Density	.0286 lb./ft.^{3}
T_a = Temperature	411.4°R, (228.56°K)
Speed of Sound	992 ft./sec.

[redacted]

Diffuser Calculations

The stagnation temperature of the air leaving the diffuser is the flight stagnation temperature and may be determined by means of the relation.

$$T_{o_1} = T_a \left(1 + \frac{k-1}{2} M^2\right) = (411.4)\left[1 + (.2)(.9)^2\right] = 477^\circ R \quad (1)$$

The actual exit stagnation pressure is determined by the equation

$$p_{o_1} = p_a \left[\eta_D \frac{k-1}{2} M^2 + 1\right]^{\frac{k}{k-1}} = (4.36)\left[(0.9)(0.2)(0.9)^2 + 1\right]^{3.5}$$

$$= 7.0 \text{ psia} \quad (2)$$

The stagnation density is found from the equation of state

$$\rho_{o_1} = \frac{p_{o_1}}{RT_{o_1}} = .0896 \text{ lb./ft.}^3 \quad (3)$$

Compressor Calculations

The compressor is in two units, separated by an intercooler. A stagnation pressure ratio of 6.5 for each compressor unit and an allowance of 5% pressure drop in the intercooler results in an overall compressor pressure ratio of 40. Consequently, the stagnation pressure at the exit of the front compressor, p_{o_2}, is 45.51 psia, and the stagnation pressure at the exit of the rear compressor is 281 psia. The stagnation temperature at the compressor outlet is calculated by the methods outlined in Kennan and Kaye's "Air Tables". For a compressor temperature rise ratio of 0.835, the exit stagnation temperature from the forward compressor is found to be 876°R (486°K). The intercooler has an effectiveness of 0.5, hence the stagnation temperature at the entrance to the rear compressor is

$$T_{o_3} = T_{o_1} - \frac{(T_{o_2} - T_{o_1})}{2} = 876 - \frac{(876 - 477)}{2} = 676.5^\circ R$$

The corresponding inlet pressure is

$$p_{os} = 0.95\ (p_{oe}) = 0.95\ (45.51) = 43.2 \text{ psia}$$

Using these values, the stagnation temperature of the air leaving the rear compressor, T_{o_4}, is found to be 1242°R.

The isentropic enthalpy increase corresponding to the stagnation pressure rise across a reversible compressor is obtained from the Keenan and Kaye Tables:

Compressor	Isentropic Enthalpy Rise
Front	80.8 Btu./lb.
Rear	114 Btu./lb.

For an overall efficiency of 0.82, the power required by the compressor is

$$\frac{80.8 + 114}{.82} = 237 \text{ Btu/lb.}$$

Reactor Calculations

The pressure loss in the ducting and reactor is 30%. Hence, the stagnation pressure at the turbine inlet is 0.7 (281) = 196.7 psia. The air is heated in the reactor to 2260°R. The method of calculating the reactor dimensions for a given maximum reactor wall temperature and a given free-flow ratio is described in Appendix III-E.

Turbine Calculations

The turbine efficiency is 87%. The turbine power is equal to the power absorbed by the compressor. Hence, the actual enthalpy drop across the turbine is 237 Btu./lb. and the enthalpy drop for an isentropic turbine expansion to the same back pressure would be $\frac{237}{.87} = 273$ Btu./lb.

Utilizing the Keenan and Kaye Tables, it is found that this enthalpy change corresponds to a turbine exit pressure of 19.2 psia and a turbine pressure ratio of 10.2. The stagnation temperature of the air leaving the turbine is found to be 1391°R.

Exhaust Duct Calculations

In the exhaust duct the air undergoes adiabatic expansion to ambient pressure (4.36 psia). The isentropic enthalpy change is 116.7 Btu./lb. The nozzle efficiency is 0.9, hence the effective enthalpy change is 105 Btu./lb. The corresponding exit velocity is 2290 ft./sec.

 [redacted]

Calculation of Specific Impulse

The specific impulse is

$$I = \frac{2290 - (992)\ (0.9)}{32.174} = 43.0\ \frac{\text{lb.-sec.}}{\text{lb.}}$$

[redacted]

[redacted]

APPENDIX III

Section B

ANALYSIS OF HELIUM GAS-TURBINE COMPRESSOR-JET

A complete performance study of the helium gas-turbine compressor jet would involve a great many calculations similar to the following, in which the methods used are illustrated for a given set of parameters (Case VII). The assumptions, especially those used in the heat-exchanger calculations, are somewhat simplified, but they serve the purpose of a preliminary evaluation. The subscripts are in reference to Figure III-4.

Assumed Conditions

The sample calculations were made for the following conditions:

Flight Altitude	30,000 feet	
Flight Mach number	0.90	
Helium compressor inlet temperature	(T_b)	200°F (660°R)
Helium compressor pressure ratio	(r_c)	4:1
Helium compressor efficiency	(η_{c_H})	0.85
Helium turbine inlet temperature	(T_d)	1800°F (2260°R)
Helium turbine expansion ratio	(r_T)	3.6:1
Helium turbine efficiency	(η_T)	0.88
Air compressor efficiency	(η_{c_A})	0.85
Heat exchanger tube diameter	(air side)	0.125 inch
Mean Mach No. of air in tubes	$(\overline{M})$	0.20
Heat exchanger free-flow ratio	(FFR)	0.50
Ratio of helium flow to air flow	$\left(\frac{w_H}{w_A}\right)$	0.13
Diffuser efficiency		0.90
Nozzle efficiency		0.92

Helium was taken as a "perfect gas", with molecular weight 4.00, specific heat at constant pressure (C_{p_H}) 1.25 Btu/lb.°F, and ratio of specific heats (k) 1.667.

Air was taken as a "perfect gas", with molecular weight 29.0, speci-

[redacted]

fic heat at constant pressure (C_{p_A}) 0.240 Btu/lb.°F, and ratio of specific heat (k) 1.400.

Helium Cycle

The helium cycle, since it is a closed perfect-gas cycle, is itself independent of such considerations as flight speed, flight altitude, and pressure level. From the assumed conditions, the efficiency, work ratio, and specific helium flow of the cycle can easily be calculated.

The helium temperature rise in the compressor (all conditions are stagnation conditions) is given by

$$T_c - T_b = \frac{T_b}{\eta_{c_H}} \left[r_{c_H}^{\frac{k-1}{k}} - 1 \right] = \frac{660}{0.85} \left[(4)^{0.400} - 1 \right] = 576°F$$

So,

$$T_c = 776°F \ (1236°R)$$

and the work of compression is

$$(T_c - T_b)C_{p_H} = (576)(1.25) = 720 \text{ Btu/lb.}$$

Similarly, the turbine temperature drop is

$$T_d - T_a = \eta_{T_H} T_d \left[1 - \left(\frac{1}{r_{T_H}} \right)^{\frac{k-1}{k}} \right] = 0.88(2260) \left[1 - \frac{1}{3.6}^{0.400} \right]$$
$$= 799°F$$

Therefore,

$$T_a = 1001°F (1461°R)$$

and the turbine work is

$$(T_d - T_a)C_{p_H} = (799)(1.25) = 999 \text{ Btu/lb.}$$

The net work available to drive the air compressor is then

$$(999 - 720), \text{ or } 279 \text{ Btu/lb.}$$

The reactor heat input is given by

$$(T_d - T_c)C_{p_H} = (2260 - 1236)(1.25) = 1280 \text{ Btu/lb.}$$

Thus, for this cycle, the characteristic parameters are

$$\text{Thermal efficiency} = \frac{\text{net work}}{\text{heat input}} = \frac{279}{1280} = 0.218$$

$$\text{Work ratio} = \frac{\text{net work}}{\text{turbine work}} = \frac{279}{999} = 0.279$$

$$\text{Specific helium flow} = \frac{\text{helium flow rate}}{\text{net power}} = \frac{1}{279} = \frac{\text{lb./hr.}}{\text{Btu/hr.}}$$

$$= \frac{1}{279}(2545)(1000) = 9140 \frac{\text{lbs./hr.}}{\text{1000 horsepower}}$$

Propulsive Duct

The temperatures and flow rate calculated for the helium cycle can now be incorporated into the propulsive duct calculation, with calculations based on the assumed helium-to-air flow ratio of 0.13. For convenience, the calculations will be made in terms of 1000 horsepower delivered from the helium cycle to the air compressor.

As in Appendix III-A, the stagnation temperature of the air leaving the diffuser is

[redacted]

$$T_{o_2} = T_{o_1} = T_1\left(1 + \frac{k-1}{2} M_1^2\right) = (411.4)[1 + (.2)(.9)^2] = 478°R$$

Defining the diffuser efficiency as

$$\eta_D = \frac{T_{2\,isentropic} - T_1}{T_2 - T_1},$$

it follows that the diffuser pressure ratio is

$$\frac{p_2}{p_1} = \left[1 + \eta_D \frac{\frac{k-1}{2}(M_1^2 - M_2^2)}{1 + \frac{k-1}{2} M_2^2}\right]^{\frac{k}{k-1}}$$

using $M_2 = 0.5$ as a reasonable axial approach velocity for the compressor,

$$\frac{p_2}{p_1} = \left[1 + 0.90 \frac{(0.2)(.81 - .25)}{1 + (0.2)(.25)}\right]^{3.5} = 1.378$$

For $p_1 = 628$ psf, p_2 865 psf, and

$$p_{o_2} = p_2\left(1 + \frac{k-1}{2} M_2^2\right)^{\frac{k}{k-1}} = 1025 \text{ psf}$$

From the equation of state, the density at the compressor inlet is

$$\rho_2 = \frac{p_2}{RT_2} = \frac{p_2\left(1 + \frac{k-1}{2}\right)M_2^2}{RT_{o_2}} = \frac{(1.05)(865)}{(53.3)(478)} = 0.0356 \frac{\text{lb.}}{\text{ft}^3}$$

The approach velocity for the compressor is

$$V_2 = M_2 C_2 = 49.1\, M_2\sqrt{T_2} = (49.1)(0.5)\sqrt{\frac{478}{1.05}} = 524 \frac{\text{ft.}}{\text{sec.}}$$

[redacted]

For the assumed $\frac{w_H}{w_A} = 0.13$, the airflow is

$$w_A = \frac{9140}{(0.13)(3600)} = 19.5 \ \frac{\text{lb.}}{\text{sec.}}$$

The compressor flow area is then

$$A_2 = \frac{w_A}{\rho_2 V_2} = \frac{19.5}{(0.0356)(524)} = 1.05 \ \text{ft}^2.$$

The compressor frontal area, which is a quantity of considerable interest, can be approximated by $A_C \approx 1.8\ A_2$, which would correspond to a ratio of blade length to pitch diameter of about 0.2. Thus, $A_C \approx 1.89$ sq. ft.

For the compressor, the inlet stagnation temperature and pressure are known, as are the work delivered to the compressor and the isentropic efficiency; the leaving stagnation temperature and pressure can be found readily, as follows.

From energy considerations,

$$T_{o_3} - T_{o_2} = \frac{\text{compressor work per pound of air}}{C_{p_A}}$$

$$= \frac{(1000)(2545)}{(0.240)(19.5)(3600)} = 151\ ^{\circ}\text{F};$$

Now, $$\frac{p_{o_3}}{p_{o_2}} = \left[1 + \frac{\eta_{C_A}(151)}{T_{o_2}}\right]^{\frac{k}{k-1}} = \left[1 + \frac{(0.85)(151)}{478}\right]^{3.5} = 2.30,$$

and $p_{o_3} = (2.30)(1025) = 2360$ psf.

For the heat exchanger, it is assumed that the Mach number through the tubes is low enough so that compressibility effects may be taken account of in a secondary way. Assume that the exchanger is of the shell-and-tube type, with air flowing through the tubes and helium flowing countercurrently outside of and parallel to the tubes. Assume that all resistance to heat transfer is on the air side; this assumption is optimistic, but it simplifies the calculations and is not unreasonable for a first approach.

The stagnation conditions leaving the compressor and the helium temperatures entering and leaving the exchanger are known, and it is necessary to calculate the air conditions leaving the exchanger and the exchanger's size and weight. Now, $T_{o_3} = T_{o_4}$, and $T_{o_5} = T_{o_6}$.

From energy considerations,

$$T_{o_5} - T_{o_4} = \frac{w_H}{w_A} \cdot \frac{C_{p_H}}{C_{p_A}} (T_a - T_b)$$

$$= 0.13 \left(\frac{1.25}{0.240}\right) (1461 - 660) = 542°F$$

Using a log mean temperature difference based on stagnation conditions,

$$\theta = \frac{(T_a - T_{o_5}) - (T_b - T_{o_4})}{\ln \dfrac{T_a - T_{o_5}}{T_b - T_{o_5}}} = \frac{290 - 31}{\ln \dfrac{290}{31}} = 116°F$$

For combined friction and heat transfer,

$$\frac{dp_o}{p_o} = -\frac{kM^2}{2}\left(\frac{dT_o}{T_o} + 4f\frac{dx}{D}\right)$$

Introducing $T_{o_m} = \dfrac{T_{o_4} + T_{o_5}}{2}$ and $\bar{M}^2 = \dfrac{M_4^2 + M_5^2}{2}$ and integrating approximately

$$\ln \frac{p_{o_5}}{p_{o_4}} = -\frac{k\bar{M}^2}{2T_{o_m}}(T_{o_5} - T_{o_4}) - \frac{k\bar{M}^2}{2}\left(4f\,\frac{L}{D}\right)$$

Using the Reynolds analogy,

$$\frac{h}{c_p G} = \frac{f}{2}$$

so that,

$$2\left(\frac{T_{o_5} - T_{o_4}}{\theta}\right) = 4f\,\frac{L}{D}$$

Therefore,

$$\ln \frac{p_{o_5}}{p_{o_4}} = -\frac{k}{2}\bar{M}^2\left[\frac{T_{o_5} - T_{o_4}}{T_{o_m}} + 2\,\frac{T_{o_5} - T_{o_4}}{\theta}\right]$$

Taking $\bar{M}^2 = 0.04$,

$$\ln \frac{p_{o_5}}{p_{o_4}} = -\frac{1.40}{2}\,(.04)\left[\frac{542}{900} + (2)\,\frac{542}{116}\right] = -0.281$$

and

$$\frac{p_{o_5}}{p_{o_4}} = 0.755$$

The entrance pressure loss, which is small, can be approximated satisfactorily by

$$\frac{p_{o_3} - p_{o_4}}{p_{o_3}} \approx \frac{k}{16}\bar{M}^2 \approx .0085$$

Therefore

$$p_{o_5} = (0.755)(1 - .0085)p_{o_3} = 1775 \text{ psf}$$

The flow area of the radiator can be obtained from

$$\left(\frac{w}{A_t}\right)^2 = \frac{\bar{M}^2\, kg\, p_{o_m}^{\,2}}{T_{o_m} R\left(1 + \frac{k-1}{2}\bar{M}^2\right)^{\frac{k+1}{k-1}}}$$

where

$$p_{o_m} = \frac{p_{o_4} + p_{o_5}}{2}$$

[redacted]

and

$$\left(\frac{w}{A_t}\right)^2 = \frac{(0.04)(1.40)(32.2)(2063)^2}{(900)(53.3)(1.008)^8} = 153$$

and the radiator flow area, A_t, is then

$$A_t = \frac{w}{\sqrt{153}} = \frac{19.5}{\sqrt{153}} = 1.58 \text{ sq. ft.}$$

Assuming a radiator free-flow ratio of 0.5, the frontal area of the radiator is 3.16 sq. ft.

To find the leaving pressure loss, it is best to find the leaving Mach number, M_5 first and then to calculate the pressure loss as

$$\frac{p_{o_5} - p_{o_8}}{p_{o_5}} \approx \frac{k}{8} M_5^2$$

Now, from continuity considerations,

$$\frac{M_5^2}{\bar{M}^2}\left[\frac{1 + \frac{k-1}{2}\bar{M}^2}{1 + \frac{k-1}{2}M_5^2}\right]^{\frac{k+1}{k-1}} = \frac{T_{o_5}}{T_{o_m}} \cdot \frac{p_{o_m}^2}{p_{o_5}^2}$$

from which, either by trial and error, or using a working chart, it is found that

$$M_5^2 = 0.077$$

Hence,

$$\frac{p_{o_5} - p_{o_8}}{p_{o_5}} = 0.0135$$

and

$$p_{o_8} = 1751 \text{ psf.}$$

[redacted]

The rough design of the exchanger can be completed by calculating L/D for an assumed tube diameter of D = 1/8 inch.

Using McAdams' equation for turbulent flow in smooth tubes,

$$\frac{h_D}{K} = 0.023\ (Re)^{0.8}\ (Pr)^{0.4}$$

and the energy equation

$$\frac{L}{D} = \frac{C_{p_a}\rho_m V_m}{4h} \cdot \frac{T_{o_5} - T_{o_4}}{\theta}$$

one obtains

$$\frac{L}{D} = \frac{(Pr)^{0.6}}{0.092} \cdot \frac{T_{o_5} - T_{o_4}}{\theta} \cdot \left(\frac{\rho_m V_m D}{\mu}\right)^{0.2}$$

The values of Prandtl number and viscosity, taken at T_{o_m}, are found in the Keenan and Kaye "Air Tables" as

$$Pr = 0.67 \text{ and } \mu = 1.79 \times 10^{-5}\ \frac{\text{lb.}}{\text{ft. sec.}}$$

Hence

$$\frac{L}{D} = \frac{(0.67)^{0.6}}{0.092} \cdot \left(\frac{542}{116}\right) \cdot \left(\frac{\sqrt{153} \times 10^5}{96 \times 1.79}\right)^{0.2} = 236,$$

and the tube length,

$$L = \frac{236}{96} = 2.46 \text{ ft.}$$

The number of tubes in parallel is

$$\eta = \frac{1.58}{\frac{\pi}{4}\left(\frac{1}{96}\right)^2} = 18,600$$

Assuming a wall thickness of 0.004 inches and a tube material density of 490 lbs. cu. ft. (steel), the tubes will weigh

$$W_t = 18600\ (490)(2.46)\left(\frac{.004}{12}\right)\left(\frac{\pi}{96}\right) = 245\ \text{lb.}$$

Assuming that the weight of the entire exchanger is twice the weight of the tubes alone, the exchanger will weigh 490 pounds.

After leaving the exchanger, the air returns to ambient pressure through the exhaust nozzle. The jet velocity is given by

$$V_7 = 223.8\sqrt{C_{p_a} T_{o_e} \eta_n \left(1 - \frac{p_7}{p_{o_e}}\right)^{\frac{k-1}{k}}}$$

$$= 223.8\sqrt{(0.240)(1171)(0.92)\left(1 - \frac{628}{1751}\right)^{0.286}}$$

$$= 1813\ \text{ft./sec.}$$

The net thrust is then

$$T = \frac{W_a}{g}(V_7 - V_{flight}) = 556\ \text{lb.}$$

and the reactor power for this thrust is

$$\frac{(1.25)(9140)(1024)}{3415} = 3430\ \text{kw.}$$

It is of interest to put the quantities determined on the basis of 1000 pounds of thrust. Then

$$\text{Compressor area} = \frac{1000}{556}(1.89) = 3.40\ \frac{\text{sq. ft.}}{\text{1000 lb. thrust}}$$

$$\text{Radiator frontal area} = \frac{1000}{556}(3.16) = 5.69\ \frac{\text{sq. ft.}}{\text{1000 lb. thrust}}$$

$$\text{Radiator weight} = \frac{1000}{556}(490) = 881 \frac{\text{lb.}}{1000 \text{ lb. thrust}}$$

$$\text{Number of radiator tubes} = \frac{1000}{556}(18{,}600) = 33{,}400 \frac{\text{tubes}}{1000 \text{ lb. thrust}}$$

$$\text{Reactor power} = \frac{1000}{556}(3430) = 6350 \frac{\text{kw.}}{1000 \text{ lb. thrust}}$$

$$\text{Airflow} = \frac{1000}{556}(19.5) = 35.1 \frac{\text{lb./sec.}}{1000 \text{ lb. thrust}}$$

$$\text{Helium flow} = 0.13\ (35.1) = 4.56 \frac{\text{lb./sec.}}{1000 \text{ lb. thrust}}$$

Power Plant Weights

Using the assumptions indicated in Chapter III of the final Lexington Report, the approximate power plant weights can be calculated readily. Since the air compressor for this case has a pressure ratio of 2.30, the weight of the air machinery for 1000 pounds of thrust is approximately

$$W_{air} = \left(\frac{6}{5}\right)^{0.6}\left(\frac{1}{0.0356}\right)(35.1) = 1100 \text{ lb.}$$

and the weight of the helium machinery, assuming a pressure of 1000 psia at the reactor inlet, is

$$W_{He} = (2.5)(2)(4.56)\left(\frac{660 \times 386}{250 \times 144}\right) = 161 \text{ lb.}$$

Therefore, for 1000 pounds of thrust, the weight of the power plant is

$$1100 + 161 + 881 = 2142 \text{ lb.}$$

[redacted]

The flyable shield thickness can be calculated for, as an example, an airplane of 300,000 pounds gross weight. The thrust, assuming an L/D of 15, is 200,000 pounds, and the power plant weight is then 42,800 pounds. For a design in which 0.725 of the gross weight is available for the power plant and shield, the weight available for shield is

$$W_s = 300{,}000\ (0.725) - 42{,}800 = 165{,}000,$$

or 55% of the gross weight is available for shield.

The reactor diameter needed to produce the required power, for a 5% pressure drop, for 100 pounds of uranium 235, and for a beryllia moderator, and for a maximum reactor wall temperature of 2500°F (2960°R), can be found by methods outlined in Appendix III-E. The diameter is L = D = 2.10 feet.

Neglecting the weight of the reactor core, and allowing for headers of 0.1 D at each end of the reactor, the flyable shield thickness is determined from a chart of shield thickness vs. allowable shield weight (for various reactor diameters) as 3.09 feet.

[redacted]

[redacted]

APPENDIX III

Section C

ANALYSIS OF BISMUTH TURBOJET

The analysis of the bismuth turbojet, insofar as the propulsive duct is concerned, is similar to the analysis of the helium gas-turbine compressor-jet outlined in Appendix III-B. However, since the reactor calculations show that the smallest reactor sizes compatible with uranium economy requirements can be approached with very low pressure drops, for all practical purposes the work required to circulate the bismuth is negligible. Because there is then no work linkage between the bismuth "cycle" and the turbojet, an additional degree of freedom is involved; here, contrary to the helium gas-turbine compressor-jet calculations, the binary-cycle temperatures and the air compressor pressure ratio are selected independently.

Assumed Conditions

The sample calculations were made for the following conditions (Case C):

Flight altitude	30,000 feet
Flight Mach number	0.90
Bismuth temperature entering radiator (T_a)	1740°F (2200°R)
Bismuth temperature leaving radiator (T_b)	540°F (1000°R)
Air-compressor efficiency (η_c)	0.835
Air-turbine efficiency (η_t)	0.87
Diffuser efficiency (η_d)	0.90
Nozzle efficiency (η_n)	0.90
Air compressor pressure ratio (r_c)	6:1
Air-turbine inlet temperature (T_{o_4})	1500°F (1960°R)
No intercooler	
Heat-exchanger tube diameter (air side)	0.125 inch
Mean Mach no. of air in tubes (M)	0.20

From the literature, bismuth was found to have a specific heat of 0.0363 Btu/lb.°F, and a specific gravity of 10, both fairly independent of temperature; the properties of air were as assumed in Appendix III-B.

Turbojet (Air Cycle)

For convenience, the turbojet calculations are based on an airflow of 100 lb/sec. The air properties at compressor inlet are the same as in Appendix III-B, namely

$$T_{o_2} = 478°R$$

$$P_{o_2} = 1025 \text{ psf}$$

and the compressor frontal area required to handle the 100 lb/sec. of airflow is

[redacted]

[redacted]

$$A = \frac{W}{pV} = \frac{(100)(1.8)}{(0.0356)(524)} = 9.66 \text{ sq. ft.}$$

The air conditions leaving the compressor are given by

$$T_{o_3} = T_{o_2}\left[1 + \frac{(r_c)^{\frac{k-1}{k}} - 1}{\eta_c}\right] = 478\left[1 + \frac{(6)^{0.286} - 1}{0.835}\right]$$

$$= 861\,^{\circ}R$$

$$p_{o_3} = 6(1025) = 6150 \text{ psf}$$

Since there is no intercooler, $p_{o_5} = p_{o_3}$, and $T_{o_5} = T_{o_3}$; also $T_{o_8} = T_{o_3}$ and $T_{o_7} = T_{o_8}$.

The log mean temperature difference in the heat exchanger is

$$\theta = \frac{(T_a - T_{o_7}) - (T_b - T_{o_8})}{\ln \dfrac{T_a - T_{o_7}}{T_b - T_{o_8}}} = \frac{240 - 139}{\ln \dfrac{240}{139}} = 185^{\circ}F$$

The radiator pressure drop is obtained from

$$\ln \frac{p_{o_7}}{p_{o_8}} = -\frac{k}{2} M^2 \left[\frac{T_{o_7} - T_{o_8}}{T_{o_m}} + 2\,\frac{T_{o_7} - T_{o_8}}{\theta}\right]$$

where

$$T_{o_m} = \frac{T_{o_8} + T_{o_7}}{2}$$

[redacted]

therefore

$$\ln \frac{p_{o_7}}{p_{o_6}} = -\frac{1.40}{2}(0.04)\left[\frac{1099}{1410} + 2\left(\frac{1099}{185}\right)\right] = -.356,$$

and

$$\frac{p_{o_7}}{p_{o_6}} = 0.700$$

The entrance pressure loss to the reactor is approximated by

$$\frac{p_{o_8} - p_{o_9}}{p_{o_8}} \approx \left(\frac{1.4}{16}\right) \bar{M}^2 \approx .0085$$

and

$$p_{o_7} = (0.700)(1 - .0085)p_{o_8} = 4290 \text{ psf.}$$

The radiator flow area can be obtained from

$$\left(\frac{w}{A_t}\right)^2 \cong \frac{\bar{M}^2 k g \; p_{o_m}^2}{T_{o_m} R\left(1 + \frac{k-1}{2} \bar{M}^2\right)^{\frac{k+1}{k-1}}},$$

where

$$p_{o_m} = \frac{p_{o_8} + p_{o_7}}{2}$$

Therefore

$$\left(\frac{W}{A_t}\right)^2 = \frac{(0.04)(1.40)(32.2)(521.0)^2}{(53.3)(1410)(1.049)} = 621$$

and

$$A_t = \frac{100}{\sqrt{621}} = 4.01 \text{ sq. ft.}$$

Assuming a radiator free-flow ratio of 0.5, the frontal area of the radiator is 8.02 sq. ft.

From continuity considerations, it follows that

$$M_7^2 = 0.098;$$

hence

$$\frac{p_{o_7} - p_{o_8}}{p_{o_7}} = \left(\frac{1.40}{8}\right)(0.098) = 0.0163$$

and

$$p_{o_8} = 4220 \text{ psf}$$

Using properties taken at T_{o_m} from the Keenan and Kaye "Air Tables" as Pr = 0.65 and $\mu = 2.54 \times 10^{-5}$ lb/ft.-sec,

$$\frac{L}{D} = \frac{(Pr)^{0.6}}{0.092} \cdot \frac{T_{o_7} - T_{o_8}}{\theta} \cdot \left(\frac{\rho_m V_m D}{\mu}\right)^{0.2}$$

Assuming D = 1/8"

$$\frac{L}{D} = \frac{(0.65)^{0.6}}{0.092} \cdot \left(\frac{1099}{185}\right) \cdot \left(\frac{\sqrt{621} \times 10^5}{96 \times 2.54}\right)^{0.2} = 314$$

and

$$L = \frac{314}{96} = 3.27 \text{ feet}$$

The number of tubes in parallel is

$$n = \frac{4.01}{\frac{\pi}{4}\left(\frac{1}{96}\right)^2} = 47,000.$$

and the weight of the tubes, for a tube wall thickness of 0.004 inches and a tube material density of 490 lb./cu. ft., is

$$W_t = 47,000\ (490)(3.27)\left(\frac{.004}{12}\right)\left(\frac{\pi}{96}\right) = 821 \text{ lb.}$$

The weight of the entire exchanger, approximated by twice the weight of the tubes alone, is about 1640 lb.

The temperature drop in the turbine is assumed for equal work to be equal to the temperature rise in the compressor, so that

$$T_{o_8} = T_{o_6} - (T_{o_3} - T_{o_2}) = 1960 + 478 - 861 = 1577^\circ R$$

and the pressure leaving the turbine is

$$p_{o_8} = p_{o_6}\left[1 - \frac{T_{o_6} - T_{o_8}}{\eta_T\ T_{o_6}}\right]^{\frac{k}{k-1}}$$

$$= 4220\left[1 - \frac{383}{(0.87)(1960)}\right]^{3.5} = 1730 \text{ psf}$$

The jet velocity leaving the exhaust nozzle is

$$V_{10} = 223.8\sqrt{C_{p_A}\ T_{o_8}\ \eta_n\left[1 - \left(\frac{p_{10}}{p_{o_8}}\right)^{\frac{k-1}{k}}\right]} = 2060 \text{ ft./sec.}$$

[redacted]

The net thrust is then

$$T = \frac{w}{g}\,(V_{10} - V_{flight}) = 3620 \text{ lb.}$$

Assuming that the bismuth pumping power is negligible, the reactor power is

$$w_A\, C_{p_A}\, (T_{o_7} - T_{o_8}) = (100)(0.24)(1099)\left(\frac{3600}{3415}\right) = 27{,}800 \text{ kw.}$$

Putting the quantities of interest on the basis of 1000 pounds of thrust, there are obtained:

$$\text{Compressor area} = \frac{1000}{3620}\,(9.66) = 2.66\ \frac{\text{sq. ft.}}{\text{1000 lb. thrust}}$$

$$\text{Radiator frontal area} = \frac{1000}{3620}\,(8.02) = 2.21\ \frac{\text{sq. ft.}}{\text{1000 lb. thrust}}$$

$$\text{Radiator weight} = \frac{1000}{3620}\,(1640) = 453\ \frac{\text{lb.}}{\text{1000 lb. thrust}}$$

$$\text{Number of radiator tubes} = \frac{1000}{3620}\,(47{,}000) = 13{,}000\ \frac{\text{tubes}}{\text{1000 lb. thrust}}$$

$$\text{Reactor power} = \frac{1000}{3620}\,(27{,}800) = 7680\ \frac{\text{kw.}}{\text{1000 lb. thrust}}$$

$$\text{Airflow} = \frac{1000}{3620}\,(100) = 27.6\ \frac{\text{lb./sec.}}{\text{1000 lb. thrust}}$$

$$\text{Bismuth flow} = \left(\frac{1000}{3620}\right)\left(\frac{0.240}{0.0363}\right)\left(\frac{1099}{1200}\right)(100) = 167\ \frac{\text{lb./sec.}}{\text{1000 lb. thrust}}$$

$$\text{Specific impulse} = \frac{3620}{100} = 36.2\ \frac{\text{lb. thrust}}{\text{lb./sec. airflow}}$$

Power Plant Weights

Using the assumptions indicated in Chapter III of the final Lexington Report, the approximate weights of the power plant components

[redacted]

can be calculated readily; the following figures are for 1000 pounds thrust.

The weight of the air machinery (compressor and turbine) is approximated by

$$W_{air} = 2(27.6)\left(\frac{1}{0.0356}\right)\left(\frac{13}{10}\right)^{0.6} = 1820 \text{ lb.}$$

It is assumed that the volume of the bismuth in the entire system is about one-fourth of the volume inside the radiator tubes. This is perhaps optimistic, but it is felt that this figure may be obtained through clever design. Hence

$$W_{Bi} \simeq (624)\left(\frac{2.21}{2}\right)(3.27)\left(\frac{1}{4}\right) \simeq 565 \text{ lb.}$$

Adding another 20% for ducts, the bismuth will weigh 678 pounds.

Neglecting the weight of the bismuth pump and of the reactor, the weight of the power plant for 1000 pounds of thrust is

$$\sim 453 + 1820 + 678 = 2950 \text{ lb.}$$

The flyable shield thickness can be calculated for, as an example, an airplane of 300,000 pounds gross weight. For an L/D of 15, the thrust is 20,000 pounds, and the power plant weight is 59,000 pounds. Assuming that 72.5% of the gross weight is available for power plant and shield, the weight available for shield is

$$W_s = 300{,}000\ (0.725) - 59{,}000 = 158{,}500 \text{ lb.}$$

The reactor diameter can be calculated by the methods of Appendix III-E. Assuming that the bismuth pumping power is 3% of the net thrust power, that the maximum wall temperature in the reactor is 1840°F(2300°R), and for 100 pounds of uranium 235 with a beryllia moderator, the diameter is L = D = 1.75 feet.

Neglecting the weight of the reactor and allowing 0.1 D at each end of the reactor for headers, the flyable shield thickness is found to be 3.15 feet.

[redacted]

APPENDIX III

Section D

MATERIALS FOR GAS TURBINES AND JET ENGINES

Less than a decade ago there were essentially no known alloys capable of withstanding high stresses at 1500°F (816°C) for long periods of time. About 1940 the U. S. Navy asked for materials capable of meeting the following conditions (as blade materials).

TABLE I

Temperature	Stress	Life	Creep Rate
1500°F (816°C)	20,000 psi	100 hours	
1500°F (816°C)	7000 psi		1%/100,000 hours

These physical properties were held to be the minima for materials capable of making the gas turbine a practical engine. For aircraft purposes (turbojets and turboprops) the specifications called for higher stresses for shorter times. A chemical specification calling for adequate resistance to oxidation at 1500°F (816°C) had to be met. The Army Air Forces for over ten years (prior to 1940) had pursued a high-temperature materials development program to provide suitable materials for aircraft use. Some interesting alloys suitable for superchargers were developed. Other alloys such as vitallium, stellites, inconels, etc., were in existence and might have been suitable with some modifications if they had been tested.

It is interesting to note that in 1940 there were no tried alloys capable of meeting these specifications by a factor of 1/2 of the stress. It is equally interesting that alloys are now available commercially which exceed these requirements by a very large margin at 1600°F (871°C) and almost meet them at 1700°F (927°C). On the basis of a short 8-year development program these results are extremely encouraging and speak well for future advances to alloys for 1800°F (982°C) service.

At the present time, primarily in the cobalt-base or nickel-base alloy systems, alloys are available for gas turbines and jet engines operating at 1500°F (816°C) for cobalt-base alloys and 1350°F (732°C) for nickel-base alloys. In both instances the presence of about 20% of chromium is sufficient for protection against harmful oxidation. At 1350°F (732°C) the chromium may be kept as low as 15% although the actual chromium content in either system depends on the balance of other elements present in the alloy. The presently known nickel-base alloys and probably any which will be developed in the future are restricted to a maximum operating temperature

[redacted]

of about 1500°F (816°C). Cobalt-base alloys in turn probably will not see high-stress service above about 1700°F (927°C). It means therefore that new alloys systems will have to be developed to achieve 1800°F (982°C) performance at stresses of the order shown above in the U. S. Navy gas-turbine requirements. Fortunately such work is going in the chromium and molybdenum-base systems and this work must be pursued to completion at a very early date.

In general, the purer the metal, the softer and the weaker it is. In such pure form the metal has the lowest recrystallization temperature. There are several avenues open for increasing the strength and resistance to deformation. These approaches amount to increasing the recrystallization temperatures of the base element. In general, the addition of any foreign element in small amounts increases the recrystallization temperature. Subsequent additions may or may not further increase the strength and recrystallization temperature. The presence of a second or third phase as a network is also effective in improving high-temperature strength; however, not all excess phases are effective; for example, sigma phase in chromium alloys is seldom desirable. Ageing systems are extremely effective and have been used to advantage for high-temperature strength.

On the basis of the recrystallization temperatures (based in this case on commercially pure metals cold-worked to 70% or more and annealed for about 1 hour at temperature) there are a limited number of alloy systems which offer use at 1200°F (649°C) and higher. Figure IIID-1 shows the relationship of the recrystallization temperature to the melting point.

It is presently known that iron-base alloys of low alloy content are restricted to about 1100°F (593°C) for high-stress performance. The stainless steels with about 20% chromium are usable up to about 1500°F (816°C) for reasonably high stresses and up to 2000°F (1093°C) (25 chromium-20 nickel-2 silicon) at extremely low stresses. High-stress applications are definitely limited to about 1300°F (704°C). Metal alloys are in use up to 1350°F (732°C) at high stresses (when supported by about 15% chromium). Cobalt-base alloys highly alloyed with 20 to 28% chromium as well as other elements have been in use at 1500°F (816°C) and it is anticipated that they will be applicable at 1600°F (871°C) and possible even at 1700°F (927°C) at somewhat lower stresses.

These three systems, iron, nickel and cobalt-base alloys have been developed quite extensively, and any further advances will be reasonably small. New alloy systems are needed.

According to Figure IIID-1, there are promising alloy systems in titanium, zirconium, chromium and molybdenum-base alloys. These four elements are sufficiently plentiful to permit wide use. Tungsten, tantalum and columbium also offer bases for alloy systems, but these elements are relatively scarce and at best would permit extremely restricted use.

Iron-Base Alloys

These alloys, the best of which are oxidation-resistant, by virtue

of a chromium content of about 20%, are not characterized by high strength. The best alloys in this system (19-9DL and Timken 16-25-6) are shown in Table III (5) where rupture properties are listed and Table IV (5) where creep properties are listed. Table II lists the compositions. As far as oxidation resistance is concerned even ordinary 18 chromium-8 nickel stainless steel is adequate for 1500°F (816°C). For oxidation resistance at 2000°F (1093°C) the alloy 25 chromium-20 nickel-2 silicon has seen extensive use as combusion-chamber-liner material in jet aircraft. The modification 35 nickel-15 chromium-2 silicon -- balance iron shows good oxidation resistance up to 1800°F (982°C) and resists carburization extremely well at 1800°F (982°C).

Nickel-Base Alloys

The strongest nickel base alloy is inconel X which has seen service at 1350°F (732°C) as jet-engine blade material. The alloy over-ages and loses strength and ductility rapidly at 1500°F (816°C). Nimonic 80 is also an interesting nickel base alloy of similar properties. Straight inconel offers extremely good oxidation resistance up to 2100°F (1149°C); it would also be a good material to resist carburization. None of these alloys, unfortunately, is very strong above 1350°F (732°C) for long times or above 1500°F (816°C) for reasonably short times.

The better known alloys in the nickel system are shown in Tables III and IV (5).

Cobalt-Base Alloys

Cobalt, a strategically scarce material, has yielded thus far the most valuable alloys for use at high stresses at 1500°F (816°C). The properties remain appreciably good up to 1800°F (982°C), although perhaps not good enough to permit stresses of the magnitude presently desired. In general these alloys are different from the nickel and iron-base alloys in that cobalt alloys are forgeable only with great difficulty or are not forgeable at all. Accordingly cobalt-base alloys are generally cast. There is no great disadvantage to this since cast alloys show greater strength at elevated temperatures than do the same alloys in the forged condition. The hot investment method has generally been applied with considerable success. The cobalt-base alloys (as are the nickel-base alloys) are again type alloys of quite complex structure which is not yet thoroughly understood. New advances in this system will probably not come as new alloys but appreciable advances will be made on the basis of better heat treatment of the alloys.

The better alloys in the cobalt base system are shown in Tables II, III, and IV (5).

A group of cast and forged alloys which are not cobalt, nickel or iron base might also be mentioned here. These are really severely alloyed stainless-type alloys wherein the nickel, iron, cobalt and chromium are present in about equal amounts at 20% each. Some extremely interesting

low-creep alloys have resulted in this system. The properties of these alloys are also shown in Tables II and III, and IV (5).

The interesting cobalt-base alloys are vitallium, 422-19, X-40, S-816, 73J and 111VT2-2. The interesting cobalt-chromium-nickel-iron alloys are N-155, 100NT-2 and 5-590.

Chromium-Base Alloys

Recent developments in the chromium-base alloys have been extremely encouraging and show definite promise of producing alloys suitable for use as turbine blades at 1800°F (982°C). These chromium-base alloys are mainly the chromium-molybdenum-iron type with small additions of titanium, manganese, columbium, etc. At the present moment strength values in rupture and creep are already large enough to assure use at 1800°F (982°C); however, the alloys are extremely brittle and will require developments along the lines of increasing the ductility. The best alloy thus far modified, Cm-469 (58 chromium-25 molybdenum-15 iron-2 titanium), has shown values at 1800°F (982°C) which exceed the minimum specifications given at the beginning of this section. This work is continuing at Battelle with promise of improved performance. Some fundamental work at M.I.T. has indicated the limits of the brittle alloys and will perhaps permit a better selection of elements to avoid the brittle sigma phase.

Chromium-base alloys are desirable in many respects. The alloys are lightweight and have reasonably good oxidation resistance. Furthermore, all the metallic elements used thus far are available in this country in sufficient amounts, these being chromium, manganese, iron, nickel, titanium. Attempts are under way to develop precision-casting techniques which will permit direct production of blades. Figure IIID-2 shows a log-stress or log-rupture time comparison of the best cobalt-base and nickel-chromium-cobalt-iron-base alloys with the best results obtained to date on chromium-base alloys. At 1600°F (871°C) the stress for 100-hour fracture for the best cobalt-base alloy is 26,000 psi against 43,000 psi for the chromium-base alloy. Only one incomplete value is presently available at 1800°F (982°C) on the chromium-base alloy. The value again places the chromium alloy curve far above the best alloy tested previously -- 100 NT-2. As of this date, new alloy variations using titanium have indicated even higher values at 1600°F (871°C) as shown in Figure III (5).

Molybdenum-Base Alloys

Molybdenum offers the basis of another high-temperature alloy system. This work will logically extend beyond the chromium work. Alloy systems of low enough melting point, i.e., 3450°F (1900°C) to 3630°F (2000°C), are possible.

It will of course be necessary to provide protection against oxidizing atmospheres when molybdenum is present in amounts appreciably over about 10%. However, this will depend on the expected life of the alloy. In this respect, recent developments along the line of forming molybdenum silicide coatings offer promise of utilizing high molybdenum content

alloys in oxidizing atmospheres. Some preliminary work at M.I.T. is underway to determine melting points and phases in high-molybdenum alloys prior to production of experimental alloys.

Titanium and Zirconium

The main development here has been the production of high purity titanium and zirconium. Some work has already been started on binary and low-alloy alloys in the titanium system. It is important to add that such alloys are fairly readily produced. Both of these elements may aid in the development of new improved high-temperature alloys.

Refractories for Turbine Buckets and Nozzle Blades

Many attempts have been made to replace the metal buckets in the turbine with refractory materials. The earliest work was carried out by the Germans during the war, perhaps not so much at that time to find materials superior to the metals, but to find materials as substitutes for the high-temperature alloys which were very scarce in that country. A great deal of effort in this country was directed towards the production of metals of very high creep resistance, and a really amazing improvement was reached in creep strength for alloys containing cobalt, tungsten and molybdenum. However, these metals are not plentiful, and it would be difficult to find sufficient quantities in an emergency.

It might be interesting to try to make a comparison between metals and ceramic materials at the temperature of the gas turbine. While there are excellent creep data for the high-temperature alloys, the data on refractories is very meager indeed and a great deal of work needs to be done in this field. There is indicated, however, at least a possibility of producing high-creep-strength ceramic materials for the higher temperature ranges. Some recent creep tests on pure sintered alumina indicate very slow creep below 2100°F (1150°C). It should be remembered that the density of the ceramic materials is roughly one-half that of metals, and therefore the stresses reached in the turbine blades will be that much less, giving the ceramic materials some advantage.

Some of the more promising refractories for buckets have been discussed, such as glass-free porcelains developed by the Bureau of Standards from a beryllium oxide or zirconia base. In Germany, some research was carried out on fused-quartz buckets, but it would not seem as if they would have enough advantage in temperature limit over metals to make them particularly interesting. Also metal-bonded oxides (1) and metal-bonded carbides have been suggested and tested with the idea of increasing the temperature shock resistance, but little is known of their creep values. One German turbine had the blades mounted on the inside of a rotating shell so that they would always be in compression (2). To date the most promising materials would seem to be high beryllium oxide content bodies and clay-bonded silicon carbide with a coating.

Also there has been some work done on the coating of metal buckets with a refractory enamel, mainly to reduce the oxidation (3) (4). This step would certainly not appreciably raise the creep limit.

As most of the turbine blades made from refractory materials must be very carefully dimensioned, it has been necessary in most cases to size them with diamond wheels after firing, but this is a very costly operation. Then it would seem difficult to produce as thin a trailing edge on the bucket of the refractory as it is possible to obtain with metal and therefore the overall efficiency of the turbine is somewhat decreased when using the refractory. Also, it should be remembered that the refractory bucket at room temperature is brittle and handling difficulties will be experienced.

Another serious problem is the fastening of the ceramic blades into the rotor. One method (2) tried in Germany was to ram powder between the blades and the rotor and then sinter it. Another method (1) consisted of silvering the base of the blade and then heavily plating with copper, so that on clamping a yielding layer would distribute the stresses.

In regard to the future, it will certainly be necessary to carry on more fundamental work on glass-free oxide bodies with a minimum of impurity. These would have to be tested for creep rate, fatigue, impact and heat-shock resistance. Also, the coated carbides, borides and nitrides are quite promising, and work on these should be carried out simultaneously. Basic research should be stressed for the next few years to build up a sound foundation on which to build future specific research.

Other Developments

1. Metals -- Powder Metallurgy. Conventional cold-pressing and sintering as well as hot-pressing and flash-hot-pressing research is well underway to develop alloys which may be strong and oxidation resistant, but which are of too high melting point for practical melting or which cannot be cast to shape or forged or machined. Work is underway in this field on alloys of:

(a) Chromium, such as the 60 chromium - 25 molybdenum - 15 iron alloy.

(b) Molybdenum.

(c) Cobalt-chromium.

2. Similar work at Ohio State, NACA and elsewhere is concerned with the production of cermets which are combinations of metals and ceramics (such as chromium - aluminum oxide) to produce impervious, dense bodies. In such bodies the chromium is oxidized superficially to chromium oxide which then forms a spinel with the aluminum oxide. The oxidation resistance of such bodies at 2400°F (1316°C) is very good. The strength is high; the thermal shock resistance is very much better than that of aluminum oxide; and the oxidation resistance is excellent. Porosity cannot be tolerated because this will lead to complete oxidation of the chromium, yielding a normal spinel body whose thermal shock resistance would be low.

These cermet bodies will definitely merit consideration as possible blade materials in the future. It is estimated that the strength of such chromium-aluminum oxide cermets will be high up to 2500°F (1371°C).

3. Still other avenues of approach are being investigated at the following places and offer possible material developments of use at high temperatures and high stresses:

(a) American Electrometals Corp.: Chromium boride bodies by powder methods.

(b) Kennametal Co.: Titanium carbide bonded with cobalt.

(c) Rensalaer Poly. Inst.: Cobalt-chromium alloys with added inter-metallics such as titanium oxide, silicon carbide, aluminum oxide etc. by flash-hot-sintering methods.

(d) Sintercast Corp: Liquid-metal impregnation of porous metallic or inter-metallic bodies. A stellite pressed and sintered body,for example, has the pores filled with cobalt, or a porous titanium carbide compact is soaked in vitallium to yield a solid body.

4. There appears to be little need to add that water or air-cooled blades are definitely practical and that an aluminum water-cooled bladed wheel has been run successfully by NACA at gas temperatures of 1800 to 2000°F (982-1093°C). The simplicity of design is lost, however, in construction and in installing the cooling system.

Conclusions and Recommendations

Alloys are presently available which are suitable for use at high stresses for periods of time from 100 to 1000 hours life at 1500°F (816°C). Among these alloys, primarily in the cobalt group, some are probably strong enough for 1600°F (871°C) service. The chances are that they could not be used at 1700°F (927°C) except at much lower stresses and are not usable at all at 1800°F (982°C).

Chromium-base alloys are known to have sufficient strength for use at 1800°F (982°C). However, these alloys are much too brittle and cannot be used at the present. They simply cannot be handled.

On the basis of progress made from 1940 to 1948 and on the basis of work underway on alloys of chromium base and of molybdenum base it is anticipated that 1800°F (982°C) turbine-blade materials will be available within the next 3 to 5 years.

Water-cooled or air-cooled blades can certainly be used for gas temperatures of 1800 to 2000°F (982 to 1093°C) provided the added mechanization and complications do not interfere with production. The simple solid blade, uncooled, is of course much more desirable due to the ease of engine construction.

It is recommended that additional research be undertaken on the chromium-base and molybdenum-base alloys. Data are needed on the binary and the ternary systems involving chromium-molybdenum-iron-nickel-cobalt-titanium-zirconium with additions of carbon and nitrogen.

REFERENCES

(1) Kistler, S. S. : Refractories in Turbine Blades and Miscellaneous applications. CIOS AP0413, 1946.

(2) Dewitt, G. H.: Development of Ceramic Materials for Use in Turbine Engines. CIOS AP0413, 1945.

(3) Bennett, D. G.: Ceramic Coatings and Ceramic Bodies for Aircraft Power Systems, Rep. No. 31, Department of Ceramic Engineering, University of Illinois, 1947.

(4) Plankerhorn, W. J. et al.: Specifications for the Preparation and Application of Certain High Temperature Ceramic Coatings for Aircraft Parts from Inconel Metal, Department of Ceramic Engineering, University of Illinois, 1947.

(5) Grant, Taylor and Frederickson: A Summary of Heat Resistant Alloys from 1200°F to 1800°F. Iron Age, March 18, April 8, April 15, 1948.

Table II

Composition of Typical Alloys

Alloy	C	Mn	Cr	Ni	Co	Mo	W	Ta	Cb	Others
19-9DL	.3	.6	19	9	--	1.3	--	(0.2Ti)	0.4	bal. Fe
16-25-6	.1	1.5	16	25	--	6.	--	--	--	" "
Nimonic 80	.04	.6	21	74	--	--	--	(2.4Ti)	(.6Al)	--
Iconel X	.05	.5	14.6	73.4	--	(.04Cu)	(.7Al)	(2.3Ti)	1.	6.9 Fe
S-816	.45	.6	20	20	45	4.	4	--	4	--
Vitallium	.3	1.	28	2	64	6	--	--	--	--
422-19	.4	.5	25	16	52	6	--	--	--	--
X-40	.5	.6	25	10	55	--	7	--	--	--
100NT-2	1.0	1.5	21	30	20	3	2.2	2	--	bal. Fe
111VT2-2	1.1	--	23	--	67	6	--	2	--	--
73J	.7	1.	23	6	60	6	--	2	--	--
N-155	.25	1.5	20	20	20	3	2.2	--	1	bal. Fe
S-590	.45	.6	20	20	20	4	4	--	4	" "

Table III

Stress to Rupture and Elongation Values for 10, 100, and 1000 Hours Life at Temperatures from 1200 to 1800° F

Alloy Name	Temp. °F.	10 Hrs. Psi	10 Hrs. %El.	100 Hrs. Psi	100 Hrs. %El.	1000 Hrs. Psi	1000 Hrs. %El.
19-9DL Forged	1200	70,000	7.0	60,000	4.3	50,000	2.5
	1350	60,000	4.0	35,000	4.0	20,500	4.0
	1500	17,500	5.0	13,300	4.0	10,000	3.0
16:25:6 Forged	1200	78,000	12.0	57,000	8.5	42,000	4.3
	1350	42,000	8.5	28,000	4.0	19,000	1.8
	1500	19,500	60.	13,300	35.0	9,000	20.
Nimonic 80 Forged	1200	78,000	3.	60,000	2.5	45,000	1.8
	1350	56,500	1	36,000	1	23,300	<1
	1500	23,000	13	16,300	9.5	11,800	<1
Inconel X Forged	1200	64,000	1	59,000	1.	55,000	1.5
	1350	58,000	50.	48,000	15	40,000	2.
	1500	45,000	25	29,000	11	18,500	2.6
S-816 Cast	1200	72,000	--	58,000	--	46,000	---
	1350	54,000	--	40,000	16	29,000	---
	1500	35,500	15	28,500	3	22,000	1
	1600	24,500	19	18,000	17	13,000	11
	1800	14,000	16	10,500	10	8,000	6
Vitallium Cast	1200	68,000	--	54,000	--	43,000	---
	1500	31,000	15	22,000	10	16,000	5
	1600	23,800	34	18,400	18	14,500	11
	1800	12,200	42	8,800	13	6,400	3
422-19 Cast	1500	39,500	40	30,400	23	23,500	6.6
	1600	25,000	24	19,000	6	14,700	1
	1800	14,400	27	10,100	18	7,100	2

Table III (Cont'd)

Alloy	Temp.	10 Hours Psi	10 Hours %El.	100 Hours Psi	100 Hours %El.	1000 Hours Psi	1000 Hours %El.
X-40 Cast	1200	66,000	---	55,000	---	46,000	---
	1500	34,000	30	28,000	12	23,200	7
	1600	25,000	36	21,300	19	18,500	7.5
	1800	13,300	46	11,300	24	9,800	8
100NT-2 Cast	1500	40,500	8	30,500	5	22,800	3
	1600	35,000	7	26,100	4	19,300	2
	1800	18,800	20	13,600	7	9,900	2.5
111VT2-2	1500	43,000	11	33,200	10	25,800	6
	1600	37,000	10	27,300	8	20,000	8
	1800	15,300	22	11,100	20	8,000	20
73J Cast	1350	69,000	7	52,500	7	40,500	7
	1500	43,500	14	34,800	13	28,200	10
	1600	33,500	16	26,400	11	21,000	6
	1800	18,000	20	12,800	10	9,300	3
N-155 Forged	1200	79,000	--	60,000	--	45,500	--
	1500	32,000	12	24,500	10	18,600	4
	1600	21,300	17	15,500	7	11,400	3
S-590 Forged	1200	69,000	33	52,000	35	40,000	37
	1500	25,500	18	20,000	18	15,500	10
	1600	19,000	44	14,000	28	10,500	20
CM469 Cast	1600	56,000	1	43,000	1	32,000	1
	1800	--	--	≃ 20,000	--	--	--

Table IV

Minimum Creep Rate of Heat Resistant Alloys at 1200 - 1600°F.
(Stress for Minimum Creep Rates, Percent per hour, of:)

Alloy	Temp. °F	0.001 1%/1000 Hrs.	0.0001 1%/10,000 Hrs.	0.00001 1%/100,000 Hrs.
19-9DL	1500	10,400	7,100	4,800
16-25-6	1200	21,500	14,000	9,000
	1500	8,400	5,700	3,800
Nimonic 80	1500	15,700	9,500	5,700
Inconel X	1500	19,600	12,300	7,600
S-816	1500	16,400	11,500	8,100
	1600	8,500	5,800	4,000
Vitallium	1500	11,700	7,600	4,900
422-19	1500	18,400	13,200	9,500
	1600	14,500	11,600	9,000
X-40	1500	18,500	13,700	10,200
	1600	15,700	11,700	8,700
100NT-2	1500	21,800	17,400	13,800
	1600	16,000	11,700	8,500
111VT2-2	1500	20,400	15,000	11,000
	1600	15,100	10,300	7,200
73J	1500	20,400	14,300	10,100
N-155	1500	13,800	10,300	7,800
S-590	1500	12,700	9,600	7,300

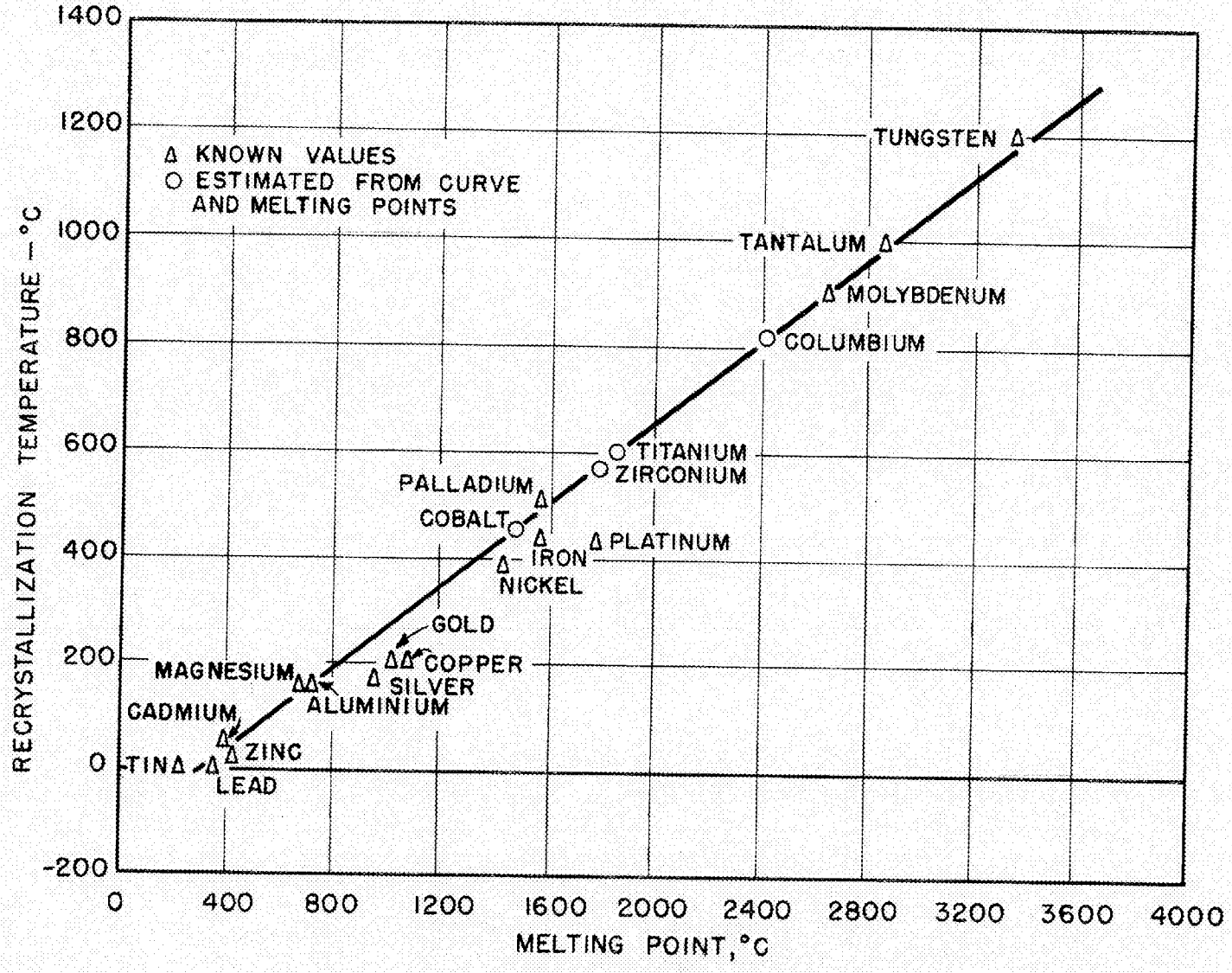

FIGURE III-D-1

FIGURE III-D-1

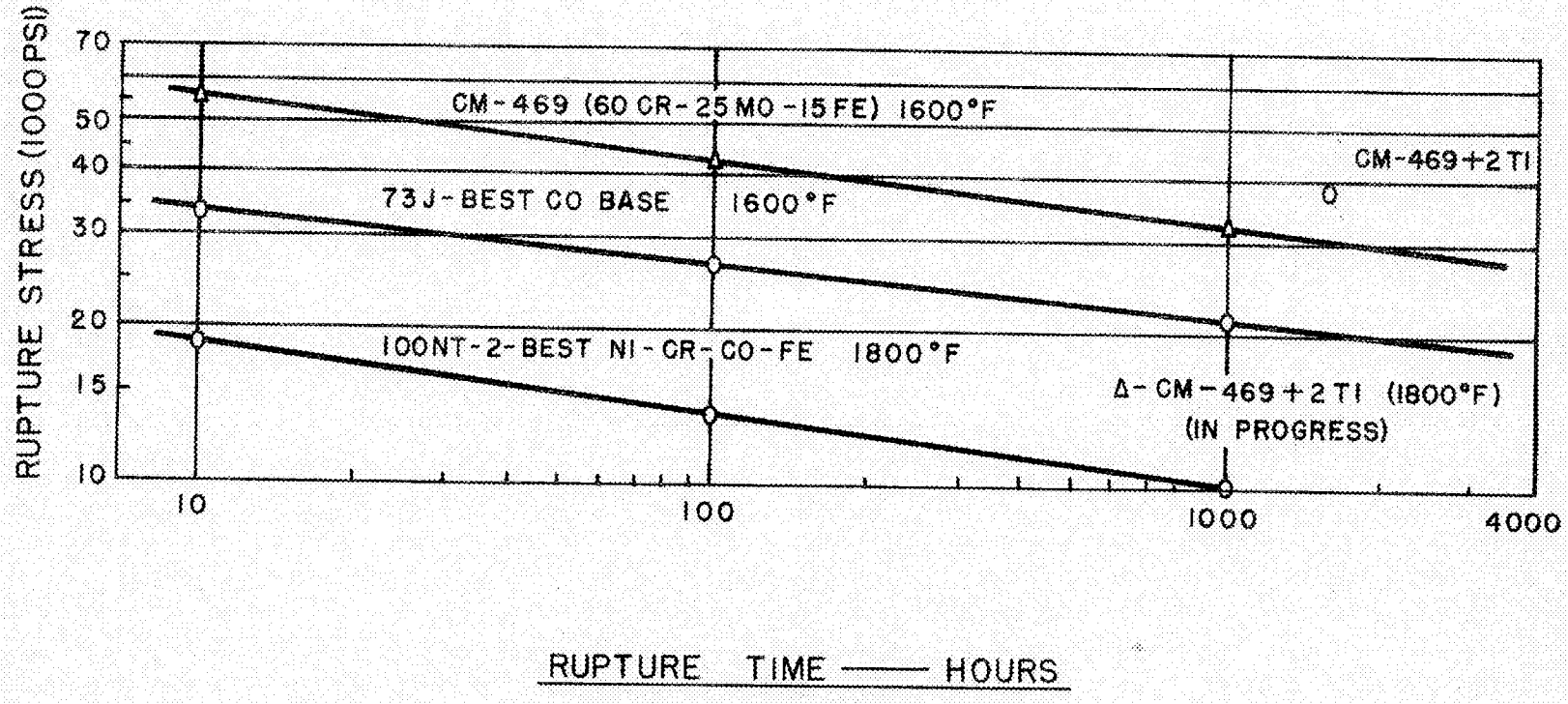

FIGURE III-D-2

FIGURE III-D-2

[redacted]

APPENDIX III

Section E

ANALYSIS OF REACTOR HEAT TRANSFER

This Appendix presents the methods used by Lexington Project personnel to analyze the problems involved in transferring heat from the reactor to a moving fluid. The treatment is not exhaustive; the intent is to indicate the theoretical basis and the techniques of calculation. The analysis is essentially one-dimensional, and hence cannot be expected to apply to all reactor heat transfer problems.

Arrangement Considered

As a representative of a cooling channel in a reactor, consider a heated passage of length L (ft.) and cross section S (sq. ft.) through which a fluid of specific heat c_p flows at the weight rate G (lb)/(sq. ft.)(sec). Let T_o (^oF.abs.) be the stagnation temperature within the passage and let T_{o4} and T_{o5} be its value at the inlet and outlet respectively. The heated length and frictional length are supposed identical.

Power Distribution

The heat input may conveniently be taken to vary along the tube in a sinusoidal manner

$$q = q_m \, \mathrm{SIN} \frac{\pi X}{(1+\theta+\sigma)L} \qquad (1)$$

where q_m is the peak heat flux in Btu/sec. ft. The symbols are defined in the Table of Nomenclature, and any dimensionally consistent set of a units may be used; those stated are for illustration only. The dimensionless parameters θ and σ serve to define the position of the sine curve

[redacted]

relative to that of the tube, as shown in Figure III-E-1. This form of distribution function permits application of the analysis to a variety of reactor configurations. Although the particular expressions set forth below are in general valid only for the power distribution of equation (1), the analysis by which they are obtained is applicable with any power distribution.

Fluid Temperature as a Function of Distance along the Passage

The first law of thermodynamics yields the relations

$$q\,dx = q_m \sin\frac{\pi x}{(1+\theta+\sigma)L}\,dx = G S c_p\,dT_o \qquad (2\text{ a})$$

$$q_m = \frac{\pi G S \bar{c}_p (T_{o5} - T_{o4})}{L(1+\theta+\sigma)\left(\cos\frac{\pi\theta}{1+\theta+\sigma} - \cos\frac{\pi(1+\theta)}{1+\theta+\sigma}\right)} \qquad (2\text{ b})$$

$$\frac{T_w - T_{o4}}{T_{o5} - T_{o4}} = \frac{\cos\frac{\pi\theta}{1+\theta+\sigma} - \cos\frac{\pi x}{1+\theta+\sigma}}{\cos\frac{\pi\theta}{1+\theta+\sigma} - \cos\frac{\pi(1+\theta)}{1+\theta+\sigma}} \qquad (2\text{ c})$$

Influence of the Maximum Temperature of the Wall of the Heated Passage

Assuming, as an approximation, the recovery factor to be unity, the heat transfer expression in the absence of a significant radiant heat flux, may be written

$$\frac{hS}{r_H}(T_w - T_o)\,dx = G S c_p\,dT_o = q_m \sin\frac{\pi x}{(1+\theta+\sigma)L}\,dx \qquad (3)$$

if r_H is the "hydraulic" radius for heat transfer, i.e., the cross section divided by the heated periphery.

For convenience of notation, let

$$\gamma = \frac{T_0 - T_{04}}{T_{05} - T_{04}} \tag{4 a}$$

$$\gamma_w = \frac{T_w - T_{04}}{T_{05} - T_{04}} \tag{4 b}$$

Then from (2 b), (2c), (3), (4 a) and (4b)

$$\gamma_w - \gamma = \frac{G\pi r_H \bar{c}_p \sqrt{1 - \left[1 - \left(1 - \frac{\cos\frac{\pi(1+\theta)}{1+\theta+\sigma}}{\cos\frac{\pi\theta}{1+\theta+\sigma}}\right)\gamma\right]^2 \cos^2\frac{\theta}{1+\theta+\sigma}}}{hL(1+\theta+\sigma)\left(\cos\frac{\pi\theta}{1+\theta+\sigma} - \cos\frac{\pi(1+\theta)}{1+\theta+\sigma}\right)} \tag{5 a}$$

$$\frac{d\gamma_w}{d\gamma} = 1 + \frac{G\pi r_H \bar{c}_p \left[1 - \left(1 - \frac{\cos\frac{\pi(1+\theta)}{1+\theta+\sigma}}{\cos\frac{\pi\theta}{1+\theta+\sigma}}\right)\gamma\right] \cos\frac{\pi\theta}{1+\theta+\sigma}}{hL(1+\theta+\sigma)\sqrt{1 - \left[1 - \left(1 - \frac{\cos\frac{\pi(1+\theta)}{1+\theta+\sigma}}{\cos\frac{\pi\theta}{1+\theta+\sigma}}\right)\gamma\right]^2 \cos^2\frac{\theta}{1+\theta+\sigma}}} \tag{5 b}$$

[redacted]

Setting $\frac{d\gamma_W}{d\gamma} = 0$ and solving for the value of γ (denoted by γ_M) which makes γ_W a maximum (denoted by γ_{WM}):

$$\gamma_M = \frac{1 \pm \dfrac{1}{\left(\cos\dfrac{\pi\theta}{1+\theta+\sigma}\right)\sqrt{1+\left(\dfrac{G\pi r_H \bar{c}_p}{hL(1+\theta+\sigma)}\right)^2}}}{1 - \dfrac{\cos\dfrac{\pi(1+\theta)}{1+\theta+\sigma}}{\cos\dfrac{\pi\theta}{1+\theta+\sigma}}} \qquad (5c)$$

The physical problem requires the minus sign in equation (5 c) to be discarded. Substituting γ_M from equation 5c for γ in equation 5a:

$$\gamma_{WM} = \left[\frac{1}{1 - \dfrac{\cos\dfrac{\pi(1+\theta)}{1+\theta+\sigma}}{\cos\dfrac{\pi\theta}{1+\theta+\sigma}}}\right]\left[1 + \frac{\sqrt{1+\left(\dfrac{G\pi r_H \bar{c}_p}{hL(1+\theta+\sigma)}\right)^2}}{\cos\dfrac{\pi\theta}{1+\theta+\sigma}}\right]$$

$$= \frac{T_{WM} - T_{04}}{T_{05} - T_{04}} \qquad (5d)$$

Equation (5 d) relates the maximum wall temperature to the fluid inlet and exit temperature, fluid mass velocity, fluid properties, heat flux distribution, and passage characteristics. A plot of γ_{WM} as a func-

[redacted]

tion of $\frac{2hL}{r_H \bar{c}_p G}$ for $\theta = \sigma = 0.0729$ is shown in Figs. III-E-2 and III-E-3

Pressure Drop

Compressible Fluids -- For a perfect gas ($pv = RT$) a combination of Newton's laws of motion and the laws of the conservation of mass and energy yields

$$\frac{dp_o}{p_o} = -\frac{kM^2}{2}\left[\frac{dT_o}{T_o} + \frac{f\,dx}{r_M}\right] \tag{6}$$

$$M = \frac{G\sqrt{T_o}\left[1 + \frac{k-1}{2}M^2\right]^{\frac{k+1}{2(k-1)}}}{p_o\sqrt{\frac{g_c k}{R}}} \tag{7}$$

where M is the Mach number in the tube, p_o is the stagnation pressure, where r_M is the hydraulic radius for flow. Equation (7) is shown graphically in Figs. III-E-4 and III-E-5.

Combining equations (2-c), (6), and (7) gives

$$-p_o\,dp_o = \frac{G^2 R\left(1+\frac{k-1}{2}M^2\right)^{\frac{k+1}{k-1}}}{2g_c}\left\{dT_o + \frac{fL}{r_M}\left[T_{o4} + (T_{o5}-T_{o1})\left(\frac{1-\dfrac{\cos\frac{\pi x}{(1+\theta+\sigma)L}}{\cos\frac{\pi\theta}{1+\theta+\sigma}}}{1+\dfrac{\cos\frac{\pi\sigma}{1+\theta+\sigma}}{\cos\frac{\pi\theta}{1+\theta+\sigma}}}\right)\right]d\left(\frac{x}{L}\right)\right\} \tag{8 a}$$

The integral of this equation from one end of the tube to the other is

$$1-\left(\frac{p_{o5}}{p_{o4}}\right)^2 = \left[\frac{T_{o5}}{T_{o4}} - 1 + \frac{fL}{r_M}\left\{1+\frac{\dfrac{T_{o5}}{T_{o4}}-1}{1+\dfrac{\cos\frac{\pi\sigma}{1+\theta+\sigma}}{\cos\frac{\pi\theta}{1+\theta+\sigma}}}\left(1-\frac{(1+\theta+\sigma)\left(\sin\frac{\pi\sigma}{1+\theta+\sigma}-\sin\frac{\pi\theta}{1+\theta+\sigma}\right)}{\pi\cos\frac{\pi\theta}{1+\theta+\sigma}}\right)\right\}\right]\Phi \tag{8 b}$$

where

$$\Phi = \frac{G^2 T_{04} R}{(p_{04})^2 g_c} \left[1 - \frac{k-1}{2} \overline{M^2} \right]^{\frac{k+1}{k-1}} \tag{9}$$

in which $\overline{M^2}$ denotes the average over the length L of the square of the Mach number. The expression in square brackets in equation (8-b) is a function solely of T_{04}, T_{05}, the power distribution, the friction factor, and the characteristics of the passage. If for example, the assumed sinusoidal heat flux distribution is symmetrical ($\theta = \sigma$) equation (8-b) may be written

$$1 - \left(\frac{p_{05}}{p_{04}}\right)^2 = \left\{ \left(\frac{T_{05}}{T_{04}} - 1\right) + \frac{fL}{r_M} \left[1 + \frac{\frac{T_{05}}{T_{04}} - 1}{2} \right] \right\} \Phi \tag{8 c}$$

<u>Evaluation of Φ</u>

For a given gas $\frac{G^2 T_{04} R}{(p_{04})^2 g_c}$ may be expressed as a function of M_4 from equation (7); plots of this function as $\frac{G\sqrt{T_0}}{p_0}$ vs. M are given for air and for helium in Figs. III-E-4 and III-E-5.

The continuity equation may be expressed in the form

$$\beta = \frac{p_{05}}{p_{04}} \sqrt{\frac{T_{04}}{T_{05}}} = \frac{M_4}{M_5} \left[\frac{1 + \frac{k-1}{2} M_5^2}{1 + \frac{k-1}{2} M_4^2} \right]^{\frac{k+1}{2(k-1)}} \tag{10}$$

which, if the reactor entrance and exit stagnation pressures and temperatures are fixed, permits M_5 to be calculated when M_4 is known. If throughout the heated section, M is less than 0.5, no serious error is introduced by evaluating $\overline{M^2}$ as the arithmetic mean of its terminal values:

[redacted]

$$\overline{M^2} = \frac{M_4^2 + M_5^2}{2} \qquad (11)$$

By combining equations (7), (9), (10), and (11), Φ may be obtained as a function of M_4 for various values of β. This function has been plotted for air (Fig. III-E-6) and for helium (Fig. III-E-7).

Pressure Drop

Liquid Coolants. Because a liquid is essentially incompressible under normal conditions of use, the pressure loss calculation for a liquid is much simpler than for a gas. In place of equation (6), for a horizontal duct:

$$p_1 - p_2 = \frac{G^2(v_2 - v_1)}{g_c} + \frac{f G^2 \bar{v} L}{2 g_c r_M} \qquad (11\ a)$$

where v_1 and v_2 are the terminal specific volumes of the liquid, $\bar{v}$ is the average of the specific volume over the length of the heated passage, and P_1, P_2 are the terminal static pressures. Unless the coefficient of expansion is very large, the quantity $(v_2 - v_1)$ will be so small that the first term on the right of equation (11a) will be negligible. Usually, therefore,

$$p_1 - p_2 = \frac{G^2 \bar{v}}{2 g_c} \left(\frac{f L}{r_M} \right) \qquad (11\ b)$$

[redacted]

Use of the Formulae

To the formulae so far assembled must first be added an agreed method of evaluating the coefficient of heat transfer h. For the cases examined, the modified Reynolds analogy

$$\frac{h}{c_p G} = \frac{\lambda f}{2} \tag{12}$$

is a good approximation. It applies sufficiently well when the flow in the channels is always turbulent and the hydraulic radii for heat transfer and for momentum transfer are identical ($r_H \approx r_M$).

The use of equation (12) permits γ_{WM} (Equation (5-d)) to be expressed as function of $\frac{\lambda f L}{r_M}$ for any specified sinusoidal power distribution:

$$\gamma_{WM} = \frac{T_{WM} - T_{04}}{T_{05} - T_{04}} = \left[\frac{1}{1 - \dfrac{\cos \frac{\pi(1+\theta)}{1+\theta+\sigma}}{\cos \frac{\pi\theta}{1+\theta+\sigma}}} \right] \left[1 + \frac{\sqrt{1 + \left(\frac{2\pi r_M}{\lambda f L (1+\theta+\sigma)} \right)^2}}{\cos \frac{\pi\theta}{1+\theta+\sigma}} \right] \tag{13}$$

A plot of this relation is shown in Figs. III-E-2 and III-E-3 for the case where $\theta = \sigma = 0.0729$. For a specified ratio of the exit to the entrance stagnation pressures for the reactor, Φ may be computed from equation (8-b). The value of M_4 may be read from a plot of Φ vs. M_4 (for instance Fig. III-E-6) at the value of $\beta = \frac{P_{05}}{P_{04}} \sqrt{\frac{T_{04}}{T_{05}}}$. The value of G may be then obtained by the use of equation (7), or from figure III-E-4.

For a given tube diameter (or hydraulic radius) of the coolant passage, the Reynolds number may be computed by using an appropriate mean viscosity of coolant:

$$N_{Re} = \frac{4 r_M G}{\bar{\mu}} = \frac{4 G S}{\bar{\mu}\ (\text{wetted Periphery})} \qquad (14)$$

The value of the friction factor for rough pipes may be read from a friction-factor plot such as the one presented in McAdam's "Heat Transmission" (1942 Edition, p. 118).

The value of λ, the correction factor in the Reynolds analogy (Equation (12)), must be evaluated in any specific case by comparing the applicable formulae or data for the friction factor f and the function $(h/c_p G)$ of the coefficient of heat transfer. For gases in turbulent flow in smooth tubes for ordinary ranges $\lambda = 1.05$ to 1.1, in commercially rough pipes a value of unity is satisfactory for ordinary calculations. For turbulent flow of liquids with viscosities near that of water, Sieder and Tate's evaluation (M. Adams "Heat Transmission", 1942 Ed., p. 168) of h, together with the following approximation for f in commercial pipes

$$f = \frac{0.0388}{(N_{Re})^{0.17} \left(\frac{\mu}{\mu_s}\right)^{0.14}}$$

gives

$$\lambda = 1.39 \left(\frac{\mu}{\mu_s}\right)^{0.28} \left(N_{Re}\right)^{-0.03} \left(\frac{c_p \mu}{K}\right)^{-\frac{2}{3}}$$

This result exemplifies the fact that λ is chiefly dependent on the physical properties of the fluid in any given case.

Illustrative Example I (Air)

Let it be required to estimate the minimum size of the reactor which is to supply power to an open-cycle turbojet and to determine its flow passages. The operating conditions for the engine are supposed specified to be:

Altitude:	30,000 ft.
Flight Mach Number:	0.90
Required Thrust:	20,000 ft.
Compressor pressure ratio:	40/1
Component efficiencies:	
Compressor, η_c	0.82
Turbine, η_t	0.87
Diffuser, η_D	0.90
Nozzle, η_N	0.90
Turbine inlet temperature:	1800°F (2260°R)
Allowable loss in absolute stagnation pressure between compressor discharge and turbine inlet:	30%

For these conditions a power plant cycle analysis by the methods of Appendix III-A yields the following figures for the state of the air leaving the compressor

Stagnation pressure	281 lb./sq.in.
Stagnation temperature:	782°F (1242°R)
Specific thrust:	43.0 lb. thrust/(lb. of air flow per sec.)

The following assumptions are made concerning the reactor:

Maximum permissible wall temperature: 2500°F (2960°R)

Ducting losses of stagnation pressure at inlet and at outlet:

1 velocity head each.

For the velocities encountered this is equivalent to pressure rations of 0.97 for the inlet ducts and 0.902 for the outlet ducts.

Reactor passages are round tubes heated over entire periphery of cross section, i.e., $r_H = r_M = d/4$

No change of stagnation temperature in entrance and exit ducts.

Symmetrical longitudinal power distribution: $\theta = \sigma = 0.0729$ (See Equation (1)); approximately uniform radial distribution

Reactor including headers is to be a square cylinder with straight one pass cooling channels parallel to the axis

Free flow cross section is 40% of reactor cross section

From the above conditions and assumptions:

$$p_{o4} = 281 \times 0.97 = 272.5 \text{ lb./sq.in.}$$

$$\frac{p_{o5}}{p_{o4}} = \frac{1 - 0.30}{0.97 \times 0.902} = 0.80$$

$$T_{o4} = 1242°R$$

$$T_{o5} = 2260°R$$

$$T_{WM} = 2960°R$$

$$\frac{T_{o5}}{T_{o4}} = \frac{2260}{1242} = 1.817$$

$$\gamma_{WM} = \frac{T_{WM} - T_{o4}}{T_{o5} - T_{o4}} = \frac{2960 - 1242}{2260 - 1242} = 1.688$$

and from Fig. III-E-2 is read

$$\frac{\lambda f L}{r_M} = \frac{2hL}{r_H \bar{c}_p G} = 2.59$$

If λ is taken to be unity, equation (8-c) may now be solved for Φ in terms of known quantities.

$$\Phi = \frac{1 - (0.80)^2}{0.817 + 2.59\left(1 + \frac{0.817}{2}\right)} = 0.085$$

By definition, (see equation (10),)

$$\beta = \frac{P_{05}}{P_{04}}\sqrt{\frac{T_{04}}{T_{05}}} = \frac{0.80}{\sqrt{1.817}} = 0.593$$

The necessary inlet Mach number for the heated passage is read from Fig. III-E-6 for these values of Φ and β :

$$M_4 = 0.231$$

The exit Mach number ($M_5 = 0.417$) may be computed from equation 10.

The required mass velocity G in the cooling channels may now be found.

From Fig. III-E-4 at the known value of M_4, is read

$$\frac{G\sqrt{T_{04}}}{P_{04}} = 0.206$$

whence

$$G = \frac{0.206 \times 272.5}{\sqrt{1242}} = 229 \text{ lb./(sq.ft.) (sec)}$$

If preferred, the same result may be obtained by computation using equation (7).

The overall dimensions of the reactor follow from the required thrust and specific impulse as soon as G is known:

Free flow cross section $= \frac{20,000}{43.0 \times 229} = 2.03$ sq. ft.

Gross cross section of reactor $= \frac{2.03}{0.40} = 5.07$ sq. ft.

Diameter of reactor $= D = \sqrt{\frac{5.07}{.785}} = 2.54$ ft.

If the header depth (t) is estimated on the hypothesis that the air is to enter radially with the same mass velocity as that in the tubes, then

$$t = \frac{\text{free flow ratio}}{4} \times D = \frac{0.40}{4} \times 2.54 = 0.254 \text{ ft.}$$

$$L = D - 2t = 0.8\ D = 2.03 \text{ ft.}$$

The diameter and number of tubular straight-through cooling channels is determinate when L is found because $\frac{\lambda f L}{r_M} = \frac{2hL}{r_H c_p G}$ has been fixed by the imposed conditions, as shown above, and all the quantities other than L in that expression either are known or are expressible in terms of the tube diameter and the physical properties of the fluid. For the present case λ has been assumed to be unity when f is evaluated for commercially rough pipes and $r_M = d/4$ if d is the diameter. Strictly, because f is usually available as a graphical function of the Reynolds number N_{Re}, a trial and error solution for d is required. However, over wide ranges f may be adequately represented by

$$f = \frac{a}{(N_{Re})^{0.17}} = \frac{a\,\mu^{0.17}}{d^{0.17}\,G^{0.17}}$$

Hence

$$\frac{L}{d^{1.17}} = \left(\frac{\lambda f L}{r_M}\right) \frac{G^{0.17}}{4\,a\,(\bar{\mu})^{0.17}}$$

Here

$$a = 0.0388$$

$$\bar{\mu} = 3.61 \times 10^{-5} \text{ lb./(ft.) (sec.)}$$

so that

$$\frac{L}{d^{1.17}} = \frac{2.59 \times (229)^{0.17}}{4 \times 0.0388 \times (3.61 \times 10^{-5})^{0.17}} = 239$$

Since L = 2.03 ft.,

$$d = \left(\frac{2.03}{239}\right)^{\frac{1}{1.17}} \times 12 = 0.204 \text{ inches}$$

The number of tubes in parallel is, therefore

$$\frac{\text{Free flow cross section}}{\text{Cross section of tube}} = \frac{2.03 \times 144}{0.785 \times (0.204)^2} = 8950 \text{ tubes}$$

As a matter of interest the Reynolds number in the tubes is

$$N_{Re} = \frac{d\,G}{\bar{\mu}} = \frac{0.204 \times 229}{12 \times 3.61 \times 10^{-5}} = 1.08 \times 10^5$$

If preferred, by means of a formulation of the heat-transfer coefficient available in terms of the Reynolds number and the physical properties, the calculation may be carried through with $\frac{2hL}{r_H \bar{c}_p G}$

regarded as the fundamental group instead of its equal $\frac{\lambda f L}{r_M}$

In this case the evaluation of Φ is the only point for which λ must be known and Φ is relatively insensitive to the value assigned to λ. When accurate heat transfer data are available, this alternative scheme is undoubtedly to be preferred.

Summary of Results of Calculations:

Reactor Diameter: 2.54 ft.

Reactor length including headers: 2.54 ft.

Header depth: 0.254 ft. = 3.05 in.

Tube length = active length of reactor: 2.03 ft.

Tube diameter: 0.204 inch

No. of tubes: 8950

Gross volume of reactor: 12.88 cu. ft.

Thrust per cu. ft.: 1533 lb./cu. ft.

The above reactor dimensions do not include any uncooled reflector.

It may be noted that this particular reactor is not necessarily practical to construct. For example, the bridge between the tubes will be less than 0.1 in. if 8950 tubes are placed in a 2.54 ft. diameter circle; this might well be impractical with the desired materials of construction. The method illustrated is intended to determine the smallest reactor from which the desired heat can be removed; in any specific case a larger size may be necessary for reasons other than heat transfer.

Illustrative Example II (Liquid Bismuth)

Let it be required to estimate the minimum size of the reactor from which the heat evolved is to be transferred to the air stream in a

propulsive duct by circulation of molten bismuth. The operating conditions for the engine are supposed to be:

Altitude:	30,000 ft.
Flight Mach Number	0.90
Required Thrust:	20,000 lb.
Compressor pressure ratio	6/1
Component efficiencies:	
Compressor, η_C	= 0.835
Turbine, η_T	= 0.87
Diffuser, η_D	= 0.90
Nozzle, η_N	= 0.90
Turbine inlet temperature:	1500°F (1960°R)

For these conditions a power plant cycle analysis by the methods of Appendix III-C yields the following figures for the required performance of the reactor:

Bismuth circulation rate:	7580 lb./sec.
Bismuth inlet temperature:	1180°F (1640°R)
Bismuth outlet temperature:	1656°F (2116°R)
Allowable loss in static head across reactor:	4.5 ft. - lb./lb.

The following assumptions are made concerning the reactor:

Maximum permissible wall temperature: 1840°F (2300°R)

Piping and header losses at inlet and at outlet:

1 velocity head each

Reactor passages are round tubes heated over entire periphery of cross section, i.e., $r_H = r_M = d/4$

No loss of temperature in entrance or exit passages.

Symmetrical power distribution: (see equation (1)); approximately uniform radial distribution.

Reactor matrix, <u>not including headers</u>, is to be a square cylinder with straight, one-pass cooling channels parallel to the axis. (Note difference from air case.)

Free flow cross-section is 40% of reactor cross section.

From the above conditions and assumptions

$T_{o4} = 1640^{o}R$

$T_{o5} = 2116^{o}R$

$T_{wm} = 2300^{o}R$

$$\gamma_{wm} = \frac{T_{wm} - T_{o4}}{T_{o5} - T_{o4}} = \frac{2300 - 1640}{2116 - 1640} = 1.386$$

and from Fig III-E-2 is read

$$\frac{2hL}{r_H \overline{c_p} G} = \frac{\lambda f L}{r_M} = 3.9$$

For the present purpose an approximation of Lyon for Martinelli's theoretical expression for the coefficient of heat transfer will be adopted (R. N. Lyon, "Pile Technology", Lecture 48 Part I, p. 20; M-4083)

$$\frac{h}{\overline{c_p} G} = \frac{1}{N_{Pe}} \left(8 + 0.02 \left[N_{Pe} - 100 \right]^{0.84} \right)$$

where

$$N_{Pe} = \frac{d G \overline{c_p}}{K}$$

If the friction factor is again taken to be adequately approximated for rough pipes by

$$f = \frac{0.0388}{\left(N_{Re}\right)^{0.17}} = \frac{0.0388 \left(\overline{\mu}\right)^{0.17}}{d^{0.17} G^{0.17}}$$

there results for λ

$$\lambda = \frac{51.5\left[8 + 0.02\left(N_{Pe} - 100\right)^{0.84}\right]}{\left(N_{Pe}\right)^{0.83}\left(\frac{c_p\,\bar{\mu}}{K}\right)^{0.17}}$$

From the International Critical Tables and the report "Some Constants for Selected Pile Materials" (ANL-WHZ-122; Oct. 1947) it is estimated for the temperature range in question that

$$\overline{c_p} = 0.0363 \text{ Btu./(lb.)(}^{\circ}\text{F)}$$

$$\bar{\mu} = 00672 \text{ lb./(ft.)(sec.)}$$

$$K = 0.00250 \text{ Btu./(sec.)(ft.)(}^{\circ}\text{F)}$$

$$K = 9.0 \text{ Btu./(hr)(ft.)(}^{\circ}\text{F)}$$

$$\frac{\bar{\mu}\,c_p}{K} = 0.00977$$

Whence

N_{Re} =	500	1000	5000	10,000	50,000
λ =	7.18	5.13	3.15	2.88	2.62

Take $\lambda = 3.5$ as a trial value because N_{Pe} is expected to be high. Then

$$\frac{fL}{r_M} = \frac{3.9}{3.5} = 1.11$$

Now, from equation (11-b), taking into account that two velocity heads are to be allowed for piping losses,

$$\frac{G^2(\bar{v})^2}{2\,g_c}\left[\frac{fL}{r_M} + 2\right] = 4.5$$

so that since $\bar{v} = 1/624$ cu. ft./lb.

$$G = \frac{64.3 \times 4.5 \times (624)^2}{(1.11 + 2)} = 6010 \text{ lb./(sq.ft.) (sec)}$$

It will be noted that G is relatively insensitive to the value estimated for λ.

The overall dimensions of the reactor follow from the required circulation rate as soon as G is known:

Free flow cross section $= \frac{7580}{6010} = 1.26$ sq.ft.

Gross cross section of reactor $= \frac{1.26}{0.40} = 3.15$ sq. ft.

Diameter of reactor, $D = \sqrt{\frac{3.15}{.785}} = 2.00$ ft.

Tube length: $L = D = 2.00$ ft.

If the header depth (t) is estimated on the hypothesis that the coolant is to enter radially with the same mass velocity as that in the tubes, then

$t = 0.10D = 0.20$ ft.

Overall Reactor Length = 2.4 ft.

When L and G are known, the tube diameter is determinate. Lyon's approximation for the heat transfer coefficient may be written

$$\frac{hK}{d\left(\overline{c_p}\,G\right)^2} = \frac{1}{\left(N_{Pe}\right)^2}\left[8 + 0.02\left(N_{Pe} - 100\right)^{0.84}\right]$$

and since $r_H = r_m = d/4$

$$\frac{hK}{d\left(\overline{c_p}\,G\right)^2} = \left[\frac{2hL}{r_H\,\overline{c_p}\,G}\right]\left[\frac{K}{8\,\overline{c_p}\,GL}\right] = \frac{3.9 \times 0.00250}{8 \times 0.0363 \times 6010 \times 2.00}$$

$$= 2.79 \times 10^{-6}$$

From a plot of Lyon's approximation (Fig. III-E-8)

$$N_{Pe} = \frac{d\,\overline{c_p}\,G}{K} = 3000$$

is read at

$$\frac{hK}{d(\overline{c_p}\,G)^2} = 2.79 \times 10^{-6}$$

At this value of N_{Pe}, λ is actually 3.5 which is fortuitously the value assumed.

Then

$$d = \frac{3000 \times 0.00250 \times 12}{0.0363 \times 6010} = 0.412 \text{ inch}$$

The number of tubes in parallel is, therefore;

$$\frac{\text{Free flow cross section}}{\text{Cross section of tube}} = \frac{1.26 \times 144}{0.785 \times (0.412)^2} = 1361$$

As a matter of interest the Reynolds number in the tubes is

$$N_{Re} = \frac{dG}{\overline{\mu}} = \frac{0.412 \times 6010}{12 \times 0.000672} = 3.07 \times 10^5$$

<u>Summary of Results of Calculations</u>

Reactor diameter: 2.00 ft.

Reactor length including headers: 2.40 ft.

Header depth: 0.200 ft. = 2.4 in.

Tube length: 2.00 ft.

Tube diameter: 0.412 in.

No. of tubes: 1361

Gross volume of reactor = 6.91 cu. ft.

Thrust per cu. ft. = 2890 lb./cu. ft.

Table of Nomenclature

A	Area of heating surface or area across which heat is flowing, sq. ft.
a	Numerical constant, dimensionless.
c_p	Specific heat, Btu./(lb.) (°F), $\overline{c_p}$ denotes average over range of temperature.
d	Tube diameter, feet; also used as differential sign.
D	Reactor diameter, feet.
f	Friction factor. (Ratio of wall shear stress to dynamic head.)
G	Fluid mass velocity, lb./(sec.) (sq. ft.)
g_c	Dimensional constant, equals $32.174 \frac{(\text{lb.-mass})(\text{ft.})}{(\text{sec.}^2)(\text{lb.-force})}$
h	Heat transfer coefficient, Btu./(sec.) (sq. ft.) (°F)
K	Thermal conductivity, Btu./(sec.) (sq. ft.) (°F/ft.)
k	Isentropic exponent, equals c_p/c_v, dimensionless.
L	Heated length of reactor passages, feet.
M	Flow Mach number in tubes = ratio of linear velocity of fluid to local acoustic velocity, dimensionless.
N_{Pe}	Peclet number, dimensionless.
N_{Re}	Reynolds' number, dimensionless.
p_o	Stream stagnation pressure, lb./sq. in. absolute.
p	Stream static pressure, lb./sq. in. absolute.
q	Heat flux per unit length of passage, Btu./(sec.)(ft.); q_m denotes the peak flux.
R	Gas Constant, $\frac{(\text{ft.})(\text{lb.-force})}{(°\text{R})(\text{lb.-mass})}$
r_H	"Hydraulic" radius for heat transfer, i.e., cross section divided by heated periphery, feet.

Table of Nomenclature (Cont.)

r_M Hydraulic radius for momentum transfer, i.e., cross section divided by wetted periphery, feet.

S Cross section of passage open for flow, sq. ft.

T_o Fluid stagnation temperature; T_{o4} denotes inlet and T_{o5} exit conditions, $^oR = {}^oF$ absolute.

T_w Wall temperature, T_{wm} denotes maximum wall temperature, $^oR = {}^oF$ absolute.

t Depth of headers of reactor, feet.

v Specific volume, cu. ft./lb.

x Distance (feet) measured in direction of flow in passage from the origin of the sinusoidal flux distribution function, see Fig. III-E-1

γ Dimensionless quantity, the fractional temperature rise

$$\gamma = \frac{T_o - T_{o4}}{T_{o5} - T_{o4}}$$

γ_w Dimensionless quantity, $\gamma_w = \dfrac{T_w - T_{o4}}{T_{o5} - T_{o4}}$

λ Dimensionless quantity in the relation $\lambda f/2 = h/c_pG$. λ is largely a function of the physical properties of the fluid.

θ Dimensionless ratio, heat flux at entrance to heated section equals

$$q_m \sin \frac{\pi\theta}{1+\theta+\sigma} \quad \text{see Fig. III-E-1.}$$

π Dimensionless number, equal to 3.1416.

σ Dimensionless ratio, heat flux at exit of heated section equals

$$q_m \sin \frac{\pi(1+\theta)}{1+\theta+\sigma} \quad \text{see Fig. III-E-1.}$$

[redacted]

Identification of Figures

Figure No.	
III-E-1	Position of heat flux distribution relative to heated passage.
III-E-2	Plot of γ_{wm} vs. $\frac{2hL}{r_H \bar{c}_p G}$ for $\theta = \sigma = 0.0729$ Low range
III-E-3	Plot of γ_{wm} va. $\frac{2hL}{r_H \bar{c}_p G}$ for $\theta = \sigma = 0.0729$ High range
III-E-4	$G\sqrt{\frac{T_o}{P_o}}$ vs. M for air.
III-E-5	$G\sqrt{\frac{T_o}{P_o}}$ vs. M. for helium.
III-E-6	Φ vs. M. for various values of β. (air)
III-E-7	Φ vs. M. for various values of β. (helium)
III-E-8	Lyons approximation of Martinelli Eq.

[redacted]

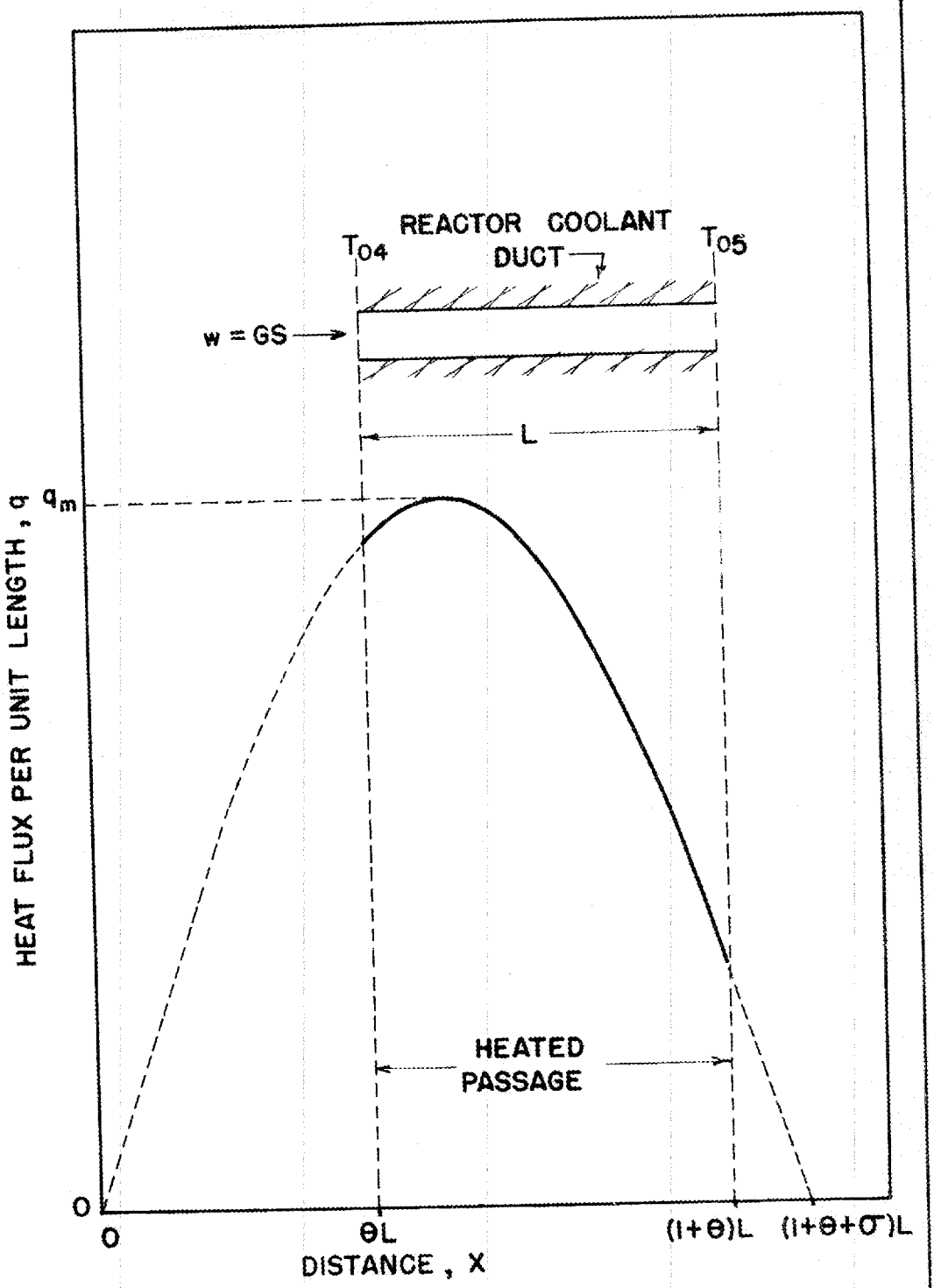

FIGURE III-E-1 GENERAL SINUSOIDAL HEAT FLUX DISTRIBUTION IN THE REACTOR.

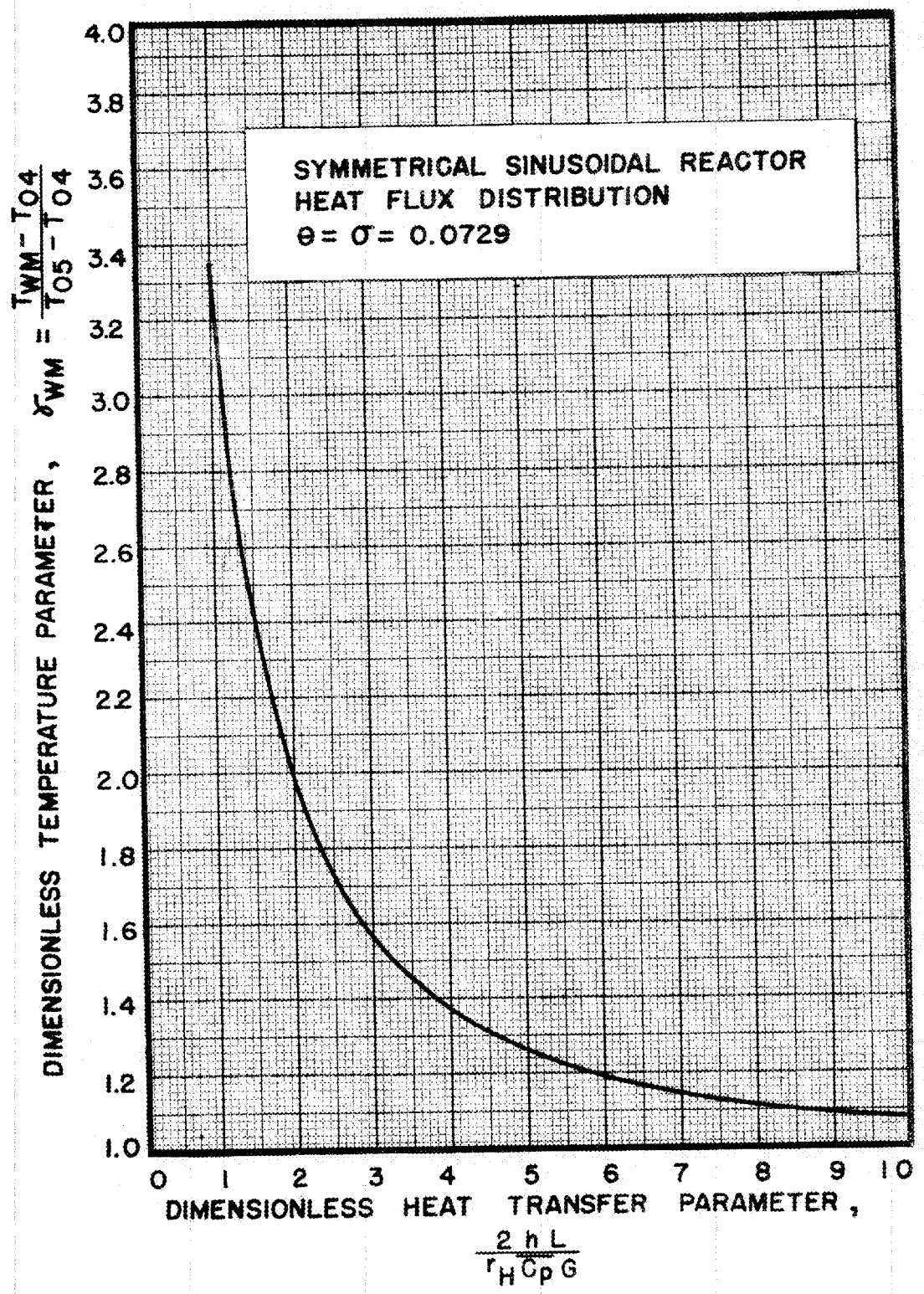

FIGURE III-E-2 CHART FOR REACTOR HEAT TRANSFER CALCULATIONS WHEN ANY COOLING FLUID IS EMPLOYED.

[redacted]

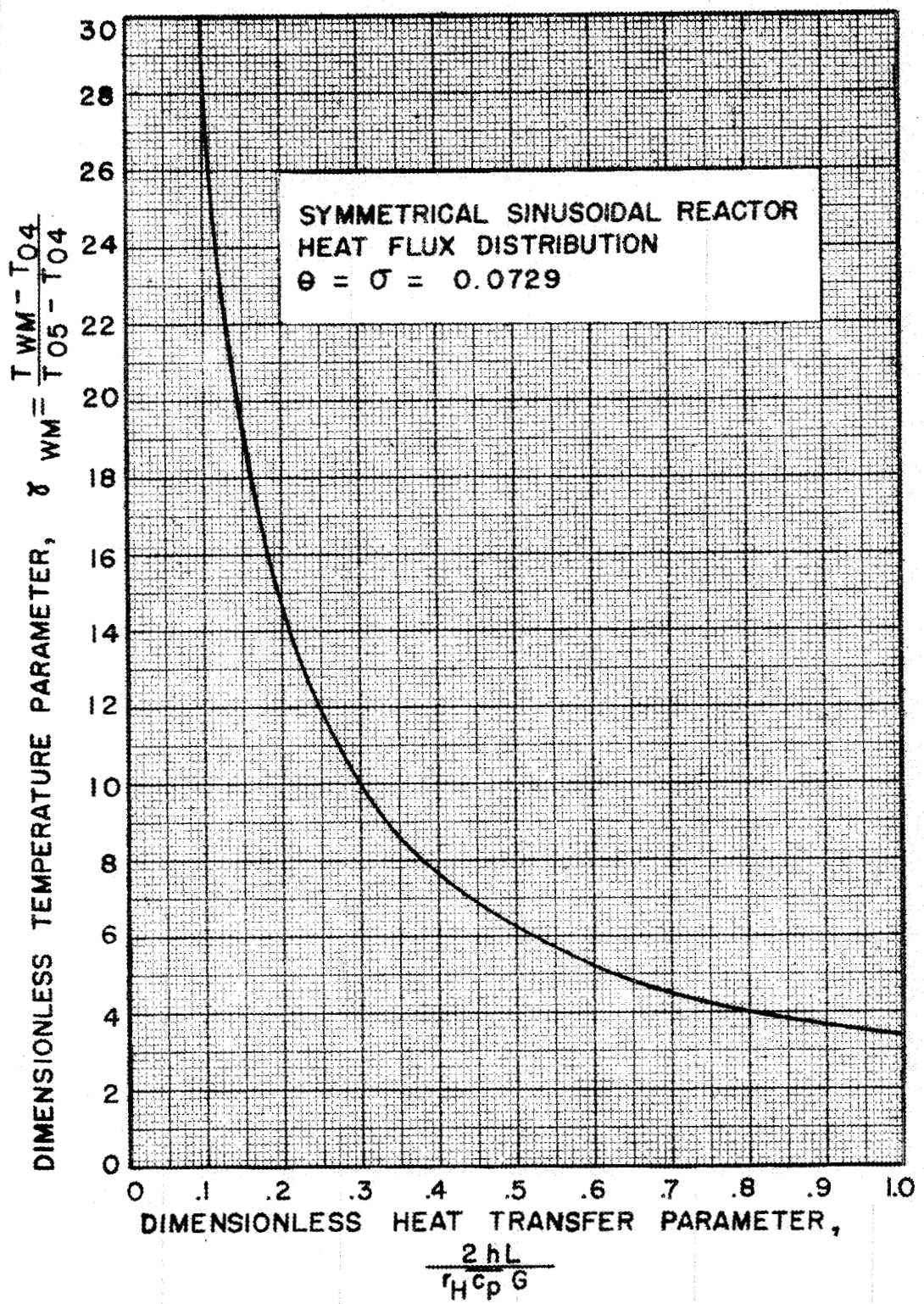

FIGURE III-E-3 CHART FOR REACTOR HEAT TRANSFER CALCULATIONS WHEN ANY COOLING FLUID IS EMPLOYED.

[redacted]

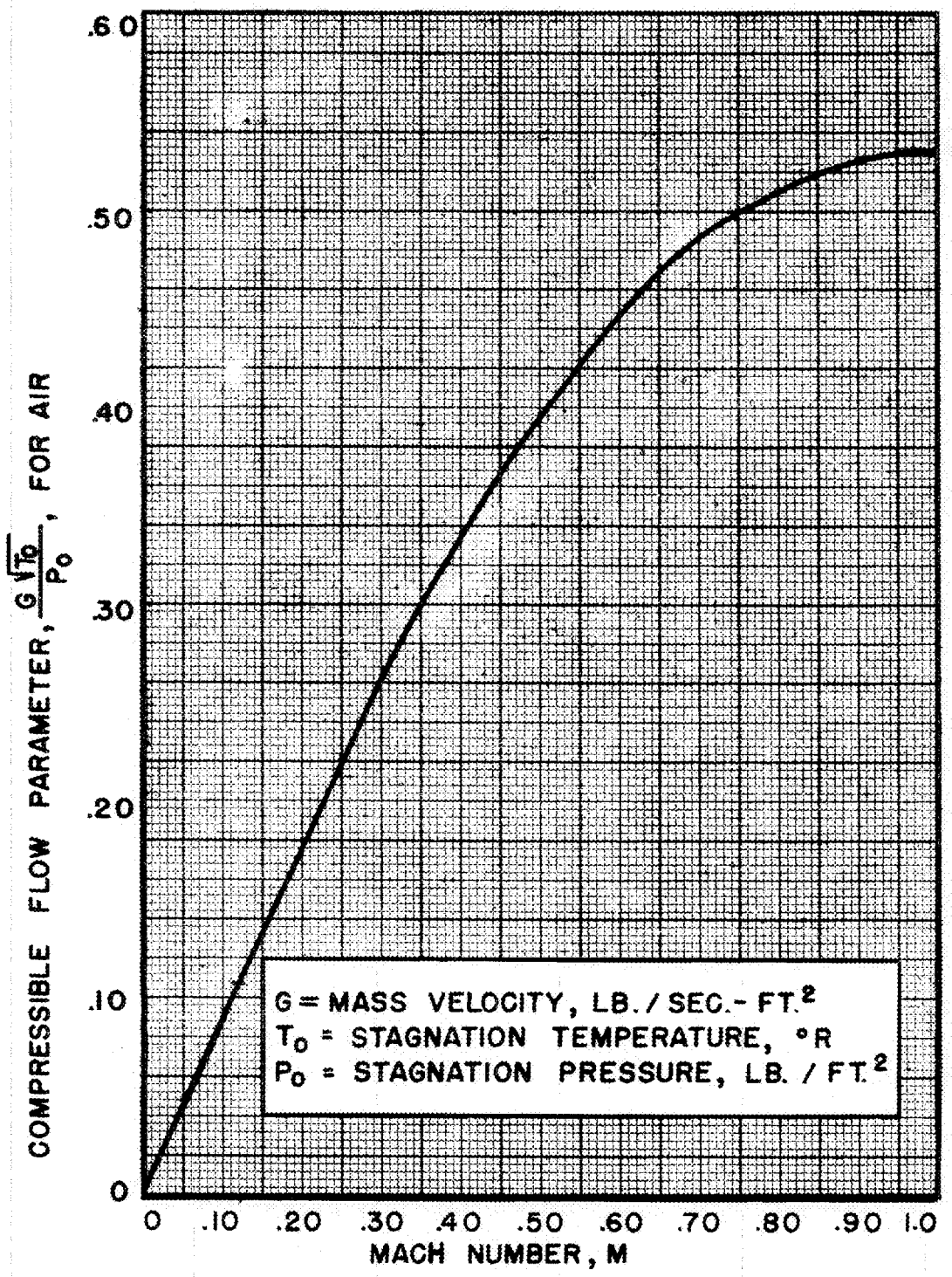

FIGURE III – E – 4 CHART FOR REACTOR HEAT TRANSFER CALCULATIONS WHEN AIR IS THE COOLING FLUID.

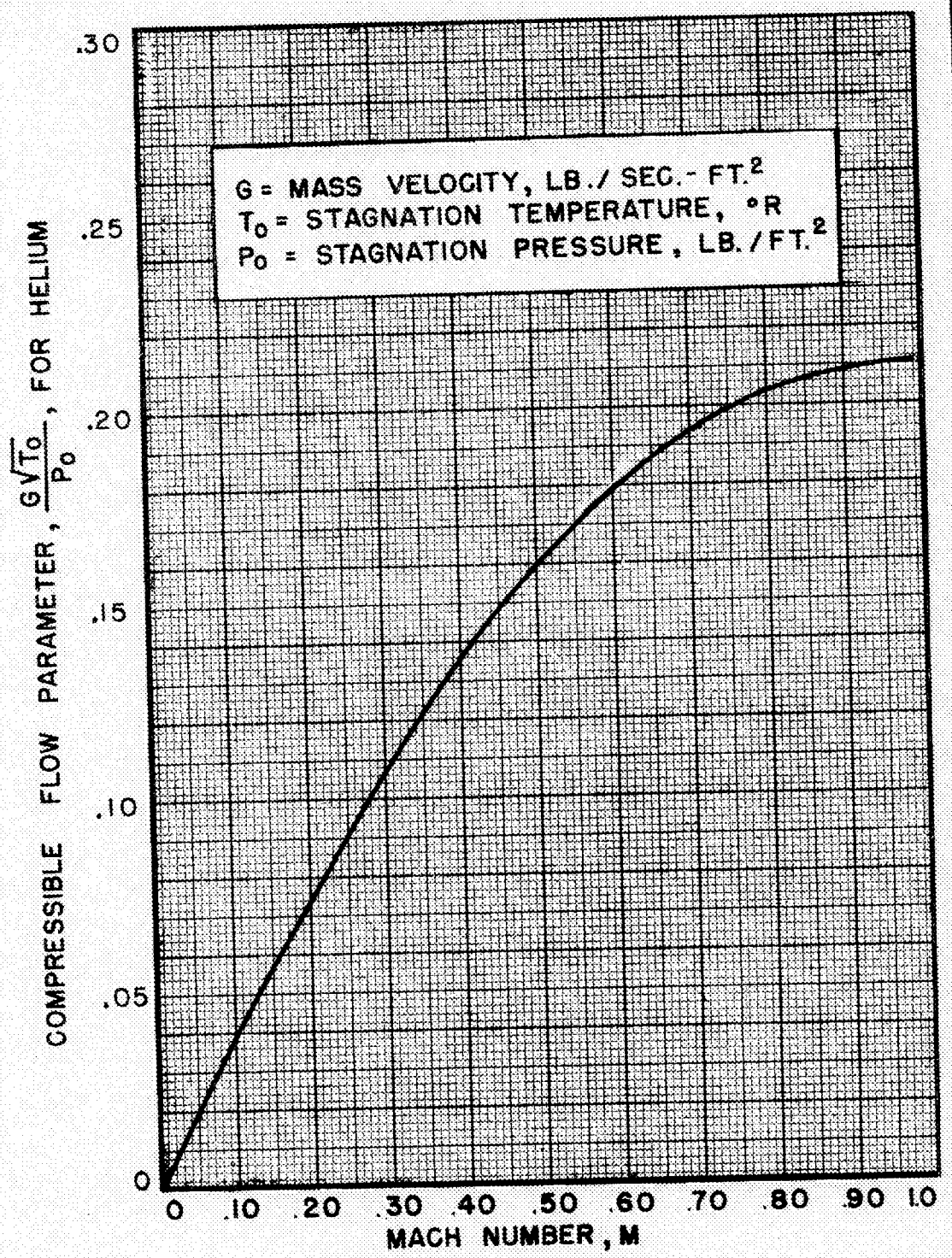

FIGURE III-E-5 CHART FOR REACTOR HEAT TRANSFER CALCULATIONS WHEN HELIUM IS THE COOLING FLUID.

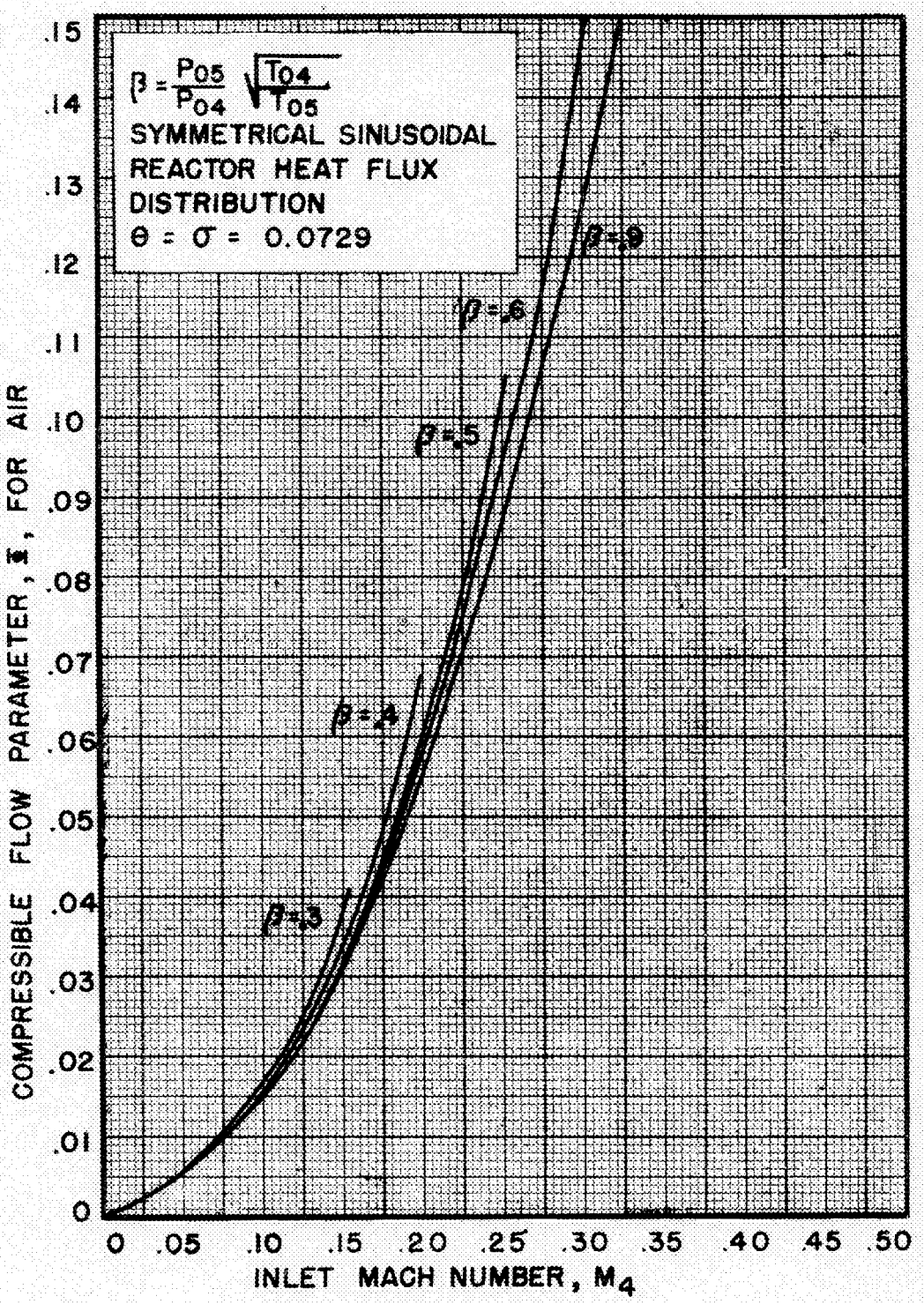

FIGURE III – E – 6 CHART FOR REACTOR HEAT TRANSFER CALCULATIONS WHEN AIR IS THE COOLING FLUID.

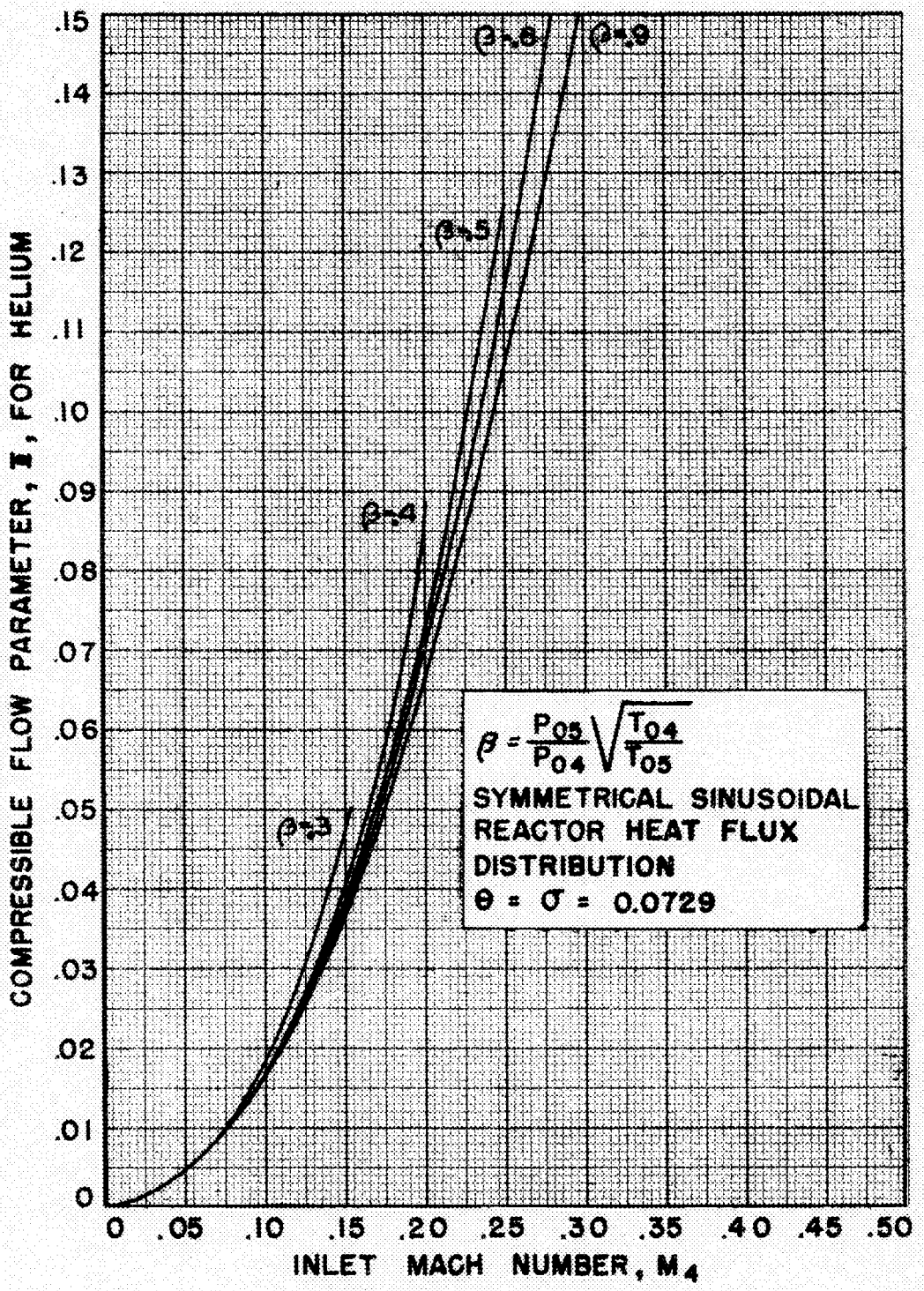

FIGURE III-E-7 CHART FOR REACTOR HEAT TRANSFER CALCULATIONS WHEN HELIUM IS THE COOLING FLUID.

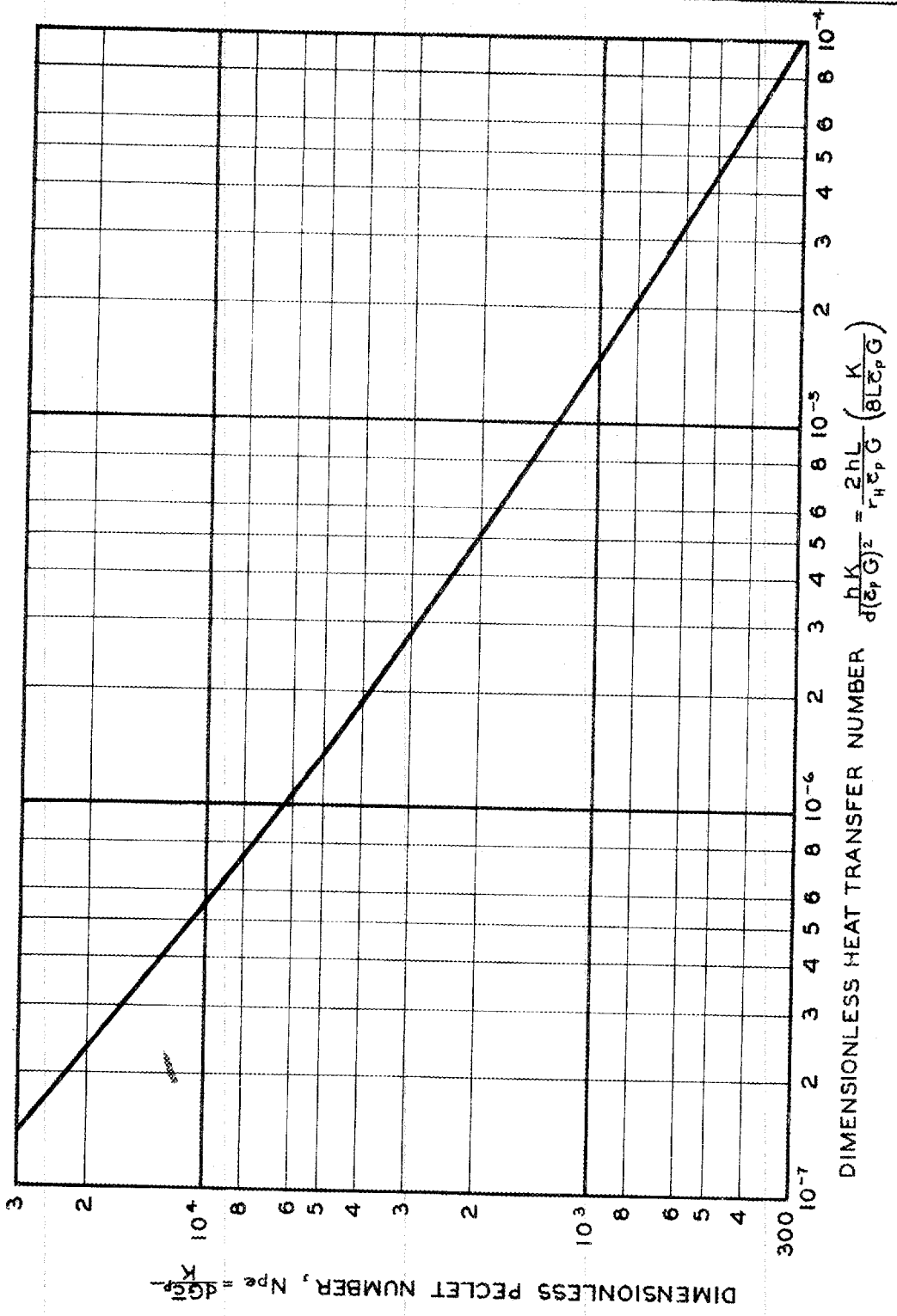

FIGURE III-E-8 LYONS APPROXIMATION OF MARTINELLI HEAT TRANSFER COEFFICIENT FOR LIQUID METALS.